Tree-ring analysis elucidating palaeo-environmental effects captured in an in situ fossil forest – The last 80 years within an early Permian ecosystem

Ludwig Luthardt[a,b,*], Ronny Rößler[a,b], Jörg W. Schneider[b,c]

[a] Museum für Naturkunde Chemnitz, Moritzstraße 20, D-09111 Chemnitz, Germany
[b] Geological Institute, Technische Universität Bergakademie Freiberg, Bernhard-von-Cotta-Straße 2, D-09599 Freiberg, Germany
[c] Kazan Federal University, 18 Kremlevskaya Str., Kazan 420008, Russian Federation

A B S T R A C T

The early Permian Chemnitz Fossil Lagerstätte (Leukersdorf Formation, Chemnitz Basin, SE Germany) represents a diverse T^0 assemblage of a fossil forest ecosystem around the Sakmarian-Artinskian transition (290.6 ± 1.8 Ma), which was preserved by pyroclastic deposits of a multi-phased volcanic eruption. The multi-aged plant community consists of predominantly hygrophilous elements, which grew on an alluvial plain mineral substrate under sub-humid conditions, representing a wet spot environment. Strong seasonality triggered the formation of annual tree rings in arborescent woody plants, such as pycnoxylic gymnosperms, medullosan seed ferns and calamitaleans. From several hundred fossil trees, the 53 best-preserved specimens were selected and investigated in detail by measuring 2,081 tree rings in individual sequences of up to 77 rings. Ring sequences were analysed by standard dendrochronological methods to determine both annual growth rates and mean sensitivity. Morphological and statistical analyses on single tree rings reveal different tree-ring types according to the different plant groups. Pycnoxylic gymnosperms have distinct and regular tree rings, whereas medullosan seed ferns and calamitaleans show indistinct and regular tree rings as well as so called event rings.

Results reveal differences between plant groups regarding their physiological reactions or adaptations to seasonal fluctuations. In comparison to pycnoxylic gymnosperms, both medullosan seed ferns and calamitaleans exhibit reduced growth rates and more sensitive reaction to environmental perturbances as water deficiency pointing to comparably lower adaptation to seasonally dry palaeoclimate. In this context, event rings are in many cases traced back to plant physiological stress during particularly severe drought periods. Altogether, these fossil trees serve as sensitive environmental archives, which shed light on growth conditions several decades back in time from the entombing eruption.

1. Introduction

Ancient in situ terrestrial ecosystems are rarely preserved in the geological record. They provide information on composition of life communities and palaeoecological processes such as organism interactions and metabolic processes (DiMichele and Falcon-Lang, 2011; Césari et al., 2012; Wang et al., 2012; Opluštil et al., 2014). Moreover, fossil ecosystems reflect their surrounding environment responding to palaeoclimate and its variations through time (Montañez et al., 2016).

Trees represent a natural data storage system, which records the biological reactions of living organisms to changes in their environment (Creber, 1977). Consequently, tree-ring analysis has become established as an important method in forestry, chronology and climatology (Schweingruber, 1996; D'Arrigo et al., 2006; Esper et al., 2012; Mbow et al., 2013; Schollän et al., 2015). In modern forest ecosystems, these

methods are applicable in many varying climatic regions of the world, ranging from the cold temperate zones to warm tropical regions (Falcon-Lang, 2005a). The formation of tree rings in individuals is often seasonally driven and influenced by both external factors such as local light and water conditions, competition pressure, underground morphology or catastrophic events, and internal factors such as genetic ability to form tree rings, ontogenetic development or inherited physiological adaptations (Creber and Chaloner, 1984; Chapman, 1994; Schweingruber, 1996; Schweingruber et al., 2006). Both internal and external factors influence growth of plants likewise and superimpose higher-ranked climatic signals. The distinction between different factors is one of the major limitations in both dendrochronology and dendroecology (Schweingruber, 1996).

Annual tree-ring formation has been questioned in tropical systems for a long time. However, this phenomenon was demonstrated in

---

modern tropical dry and wet forests by several studies during the last century, even though it differs significantly from tree-ring formation in the temperate zone (Coster, 1927, 1928; Worbes, 1995, 2002; Fichtler et al., 2003; Bräuning et al., 2009; Rozendaal and Zuidema, 2011; Groenendijk et al., 2014). Tropical climate is characterised by seasonal fluctuations of precipitation resulting in at least one dry season, whereas more than one can arise in various regions world-wide, e.g. driven by monsoonal circulation (Ash, 1983, 1985). Basically, tree-ring formation in the tropics is induced by growth interruption due to moisture stress in the dry season. Mechanisms of drought tolerance in tropical dry forests are mainly forced by species-specific plant physiological processes, which are the key factors influencing phenological behaviours, such as fall of leaves and changes in cambial activity (Borchert, 1980; Worbes et al., 2013). These processes result in widely varying appearance of annual rings in tropical trees, ranging from absent to weakly developed rings with diffuse boundaries and well developed rings with sharp boundaries (Coster, 1927, 1928). Variations commonly occur among different species in the same community, but also in the same species at different stands.

Due to their high potential for providing palaeoecological information, dendroecological methods have been applied to fossil wood, mainly petrified or charcoalified remains (e.g. Francis, 1984; Creber and Chaloner, 1985; Ash and Creber, 1992; Falcon-Lang, 1999; Brison et al., 2001; Falcon-Lang et al., 2001; Taylor and Ryberg, 2007; Pires and Guerra-Sommer, 2011; Gulbranson et al., 2014; Benício et al., 2015; Fletcher et al., 2015). However, application is generally limited due to comparatively small data bases, caused by multiple taphonomic biases such as inadequate cell preservation or fragmentation during various transport processes. Well-preserved in situ fossil forests solely provide the opportunity to avoid these biases and admit the application of modern methods usually applied to extant wood. An example is the T^0 assemblage of the Chemnitz Fossil Lagerstätte (Rößler et al., 2012). It represents a diverse fossil assemblage of early Permian age (Sakmarian-Artinskian boundary), which encompasses several arborescent plant groups of a hygrophilous plant community (Kretzschmar et al., 2008; Rößler et al., 2008, 2009, 2010). Exceptional taphonomic circumstances with T^0 burial by volcanic ashes have been demonstrated by the ongoing scientific excavations in the city of Chemnitz (Rößler et al., 2012, 2015; Luthardt et al., 2016). The in situ character of the fossil assemblage implies that the entirety of organisms found in the Zeisigwald Tuff pyroclastics and their underlying palaeosol lived simultaneously in the same habitat. This favourable condition offers the unique possibility to apply dendrochronological and dendroecological methods even to a Permian fossil forest and its arborescent woody elements. Although it was located at a low-latitude palaeogeographical position of ca. 15° N, the fossil forest grew under sub-humid local conditions (Luthardt et al., 2016) in a subtropical semi-arid climate (Roscher and Schneider, 2006; Roscher et al., 2008), suitable for tree-ring formation. Nevertheless, the existence of true tree rings in woody plants from Chemnitz has been questioned for a long time. Morgenroth (1883) described bends and kinks of radial cell columns in gymnosperm woods, which he identified as apparent tree rings. Much later, "growth rings" were recognised in calamitaleans from Chemnitz reasoning that these growth interruptions were induced by seasonality or volcanic activity (Rößler, 2006; Rößler and Noll, 2010). Recent work on these tree rings encompassed measurement of ring sequences from 43 specimens of different taxa providing a correlation of ring sequences and evidence of a regular 10.62 year cyclicity, which was interpreted as a climatic signal forced by the 11-year solar cycle (Luthardt and Rößler, 2017). Although trees represent biological data archives, which in certain cases reflect non-climatic effects (Schweingruber, 1996), the impact of sunspot cyclicity on growth patterns is highly suggestive and gets support from varved lake sediments of the Upper Oberhof Formation in the Thuringian Forest Basin, situated about 100 km west of the Chemnitz Basin. The contemporaneous Oberhof and Leukersdorf formations can be correlated and belong to the last level with perennial

lakes in the European Permian (Schneider et al., 2006, 2012; Roscher and Schneider, 2006). Lacustrine varved laminites of the Oberhof Fm. were caused by seasonal changes of wet and pronounced dry periods and assembled distinct bundles (unpublished MSc thesis Schulz, 2015; Schulz and Schneider, 2015). The numbers of varves inside the bundles vary from 5 to 14, providing a mean value of 10.4 (see Supplement 1), but these results require confirmation in detail by ongoing research. Tree rings and varves as independent lines of evidence need to be traced back to a superordinate driver, such as climate (Haltia-Hovi et al., 2007; Glur et al., 2015).

Correlation of tree-ring sequences in the Chemnitz Fossil Forest allows assessing plant growth and environmental fluctuations up to 79 years back in time from the in situ burial by volcanic ashes (Luthardt and Rößler, 2017). Additionally, for the first time we are able to recognise deadwood among specimens of the dataset (see Supplement 2).

Here we extend tree-ring data by additional specimens and shed light on growth dynamics of the different plant taxa. We specify palaeoecological conditions, under which these plants grew and how they adapted to environmental stress. The study gives further insight into high-resolution environmental fluctuations in a three-dimensionally preserved forest ecosystem, and thus further assesses its fourth dimension.

2. Geological setting

The Chemnitz Basin is situated in southeast Germany in the Federal State of Saxony. With an extension of 70 × 30 km following a NE–SW striking (Fig. 1), it is one of the smaller post-Variscan intramontaneous Rotliegend basins of Central Europe (Roscher and Schneider, 2006; Schneider et al., 2010). The basin fill is dominated by early to late Permian terrestrial red bed sediments and intercalated volcanics. Asselian to Artinskian deposits superimpose discordantly the metamorphic basement and several smaller Carboniferous basin structures. After a hiatus, Capitanian to Wuchiapingian sediments, overlain by marine and sabkha deposits of the Zechstein Sea transgression, complete the sedimentary succession (Legler and Schneider, 2008; Schneider et al., 2012). The continental Permian strata are subdivided into four formations comprising six sedimentary megacycles with an
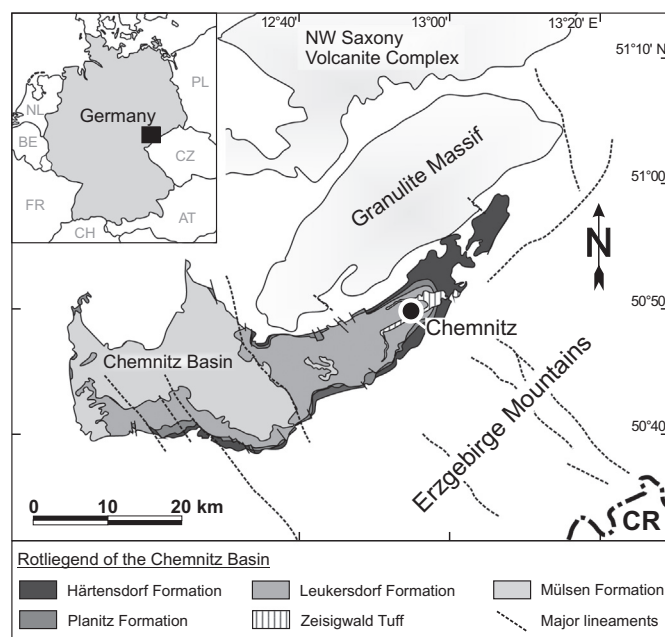

Fig. 1. Geographical position and geological setting of the working area in the Chemnitz Basin; Formation signatures show colours from dark to bright with younger stratigraphy (modified from Schneider et al., 2012).
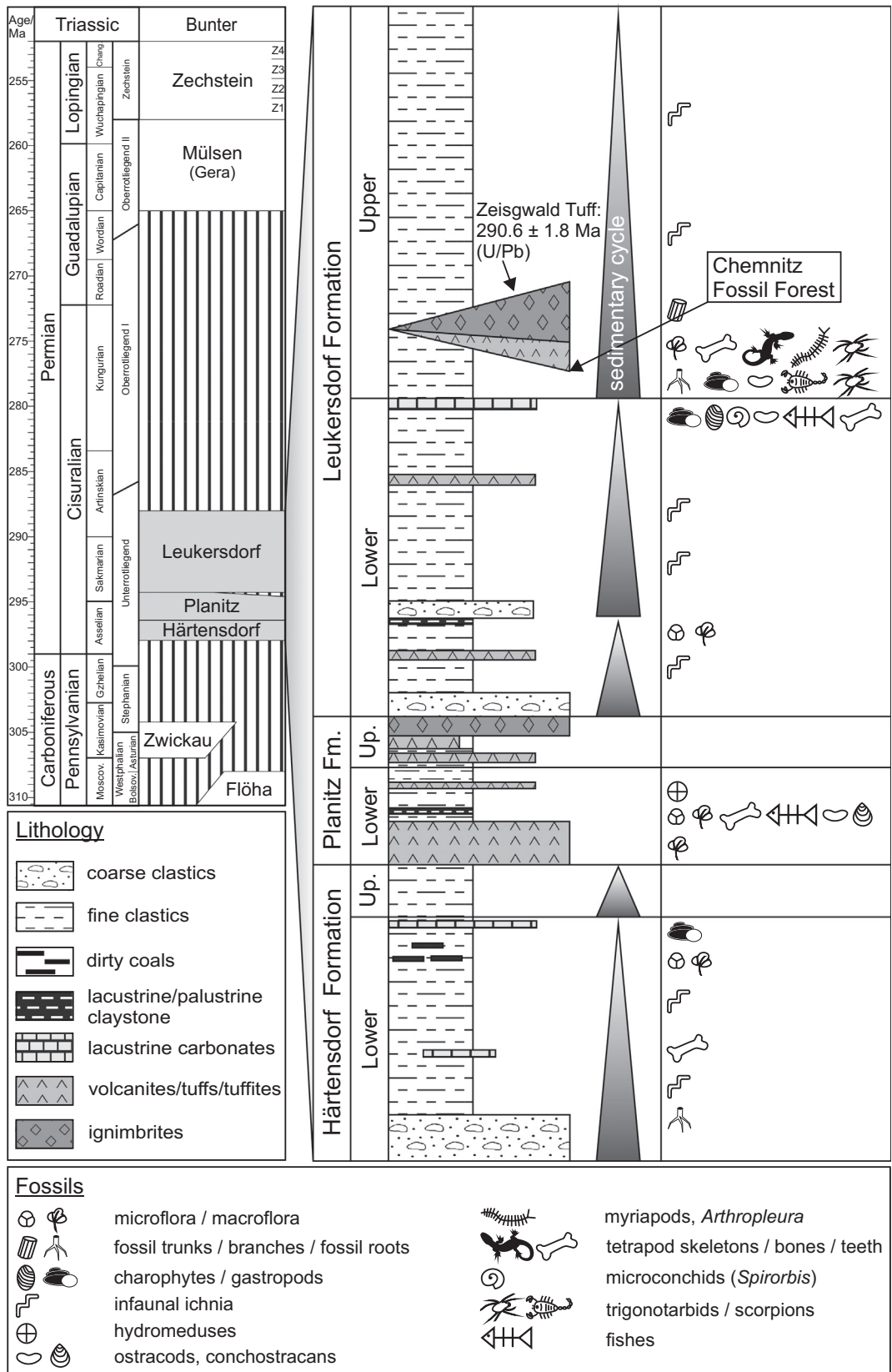
Fig. 2. Stratigraphy and lithology of early Permian terrestrial deposits of the Chemnitz Basin showing the Zeisigwald Tuff deposits in the upper Leukersdorf Formation, which host the Chemnitz Fossil Forest.

overall thickness of 1550 m (Fig. 2).

The fossil forest is located in the city of Chemnitz, in the centre of the north-eastern branch of the Chemnitz Basin. Buried by pyroclastic deposits of the Zeisigwald Tuff, it is stratigraphically part of the Upper Leukersdorf Formation (Fig. 2). The entire Leukersdorf Fm. represents an 800 m thick sequence of predominantly alluvial red-bed sediments, in which three fining-up mesocycles are subdivided, whereas the base of each cycle is defined by an initial deposition of coarse clastics of semi-arid type alluvial fans (Schneider et al., 2012). The first mesocycle is terminated by the grey-coloured lacustrine-palustrine Rottluff Horizon, the second mesocycle by the lacustrine Reinsdorf Carbonate Horizon, which shows seasonally induced lamination. Frequently, rhizolith-bearing, vertic to calcic palaeosols of low maturity as well as infaunal burrows of *Scoyenia* and *Planolites montanus* types occur in the fine- to medium-grained alluvial sediments, characterising them as "wet" red beds (Schneider et al., 2010). A basin-wide minor record of meso- to xerophilous plant remains contrasts the locally distributed hygrophilous plant assemblage of the Chemnitz Fossil Forest, which was recently characterised as a "wet spot" sensu DiMichele et al. (2006) by Luthardt et al. (2016). The Upper Leukersdorf Formation correlates with the initiation of the late Sakmarian to early Artinskian wet phase D according to Roscher and Schneider (2006).

The intercalated Zeisigwald Tuff represents a pyroclastic marker horizon in the north-eastern part of the basin (Schneider et al., 2012) and revealed an isotopic U-Pb age of 290.6 ± 1.8 Ma (Rößler et al., 2008). During intermittent ascent from a shallow magma chamber the highly evolved silicic magma came in contact with groundwater resulting in an explosive, phreatomagmatic fissure eruption, accompanied by the formation of a caldera-like structure (Eulenberger et al., 1995). Although the multi-phased character of the eruption is evidenced by a differentiated profile, it is assumed that it represents a continuous eruption without longer phases of quiescence. The earliest pyroclastics buried the forest ecosystem rapidly with ashes and flow deposits and gave rise to an exceptional in situ fossil lagerstätte revealing a diverse T⁰ assemblage (Rößler et al., 2012). A high number of trees were found still maintaining their growth positions. However, frequently observed short-distant transport phenomena were recognised at stems and branches and interpreted to be related to concentrated and diluted pyroclastic density currents.

Between 2008 and 2011, the Chemnitz Fossil Forest was investigated for the first time in a perennial scientific excavation at Chemnitz-Hilbersdorf (Kretzschmar et al., 2008; Rößler et al., 2008, 2009, 2010, 2012). Fifty-three bases of upright-standing trees were recognised at an area of 24 × 18 m, still rooting in their palaeosol, which developed on primarily deeply oxidised red alluvial plain deposits. The approximately two metres thick palaeosol horizon, Unit S6, was recently characterised in detail by Luthardt et al. (2016). It is composed of a red-coloured immature inceptisol-like, but densely rooted sub-horizon at the top, which merges into a carbonate-rich, green bleached part to the bottom (Fig. 3B). Among rooting tree bases the spectacular finding of complete scorpions in their own burrows became known recently (Dunlop et al., 2016).The uppermost sub-horizon once represented a silty to sandy, well-drained sediment, which shows minor evidence of chemical weathering. Intergrowth of carbonate and ferritic glaebules in the transition zone from the top to the bottom indicate a strongly seasonal palaeoclimate characterised by an alternation of dry and wet phases. Geochemical analyses permitted annual precipitation estimations in a range of 800 to 1100 mm (Luthardt et al., 2016). The lower, bleached part of the palaeosol frequently hosts carbonate glaebules of different size and, as witnessed by mineralogical and geochemical characteristics, a massive groundwater calcrete horizon at a depth of 0.80 to 1.10 m. Formation of this horizon probably resulted from both a high and more or less stable groundwater table and high evapotranspiration during drier seasons. A dense hygrophilous plant community comprising multi-aged medullosan seed ferns, cordaitaleans, psaroniaceous tree ferns and calamitaleans

developed on the mineral soil and was most probably supported by the high groundwater table (Luthardt et al., 2016).

The palaeosol is overlain by 0.54–0.61 m thick, fine to coarse ash deposits of the initial eruption phase, units S5 and S4 (Fig. 3B). Purple to light-grey/green-coloured, thinly bedded and unwelded, accretionary lapilli-bearing ash tuffs are interpreted as deposited from fallout with a lateral transport component. They show an internal coarsening-up, which is assumed to reflect increasing eruption energy. The lowermost horizon, S5.1, interpreted as the initial fallout of a low-energy phreatomagmatic eruption, represents the key horizon of the in situ fossil record. Numerous plant and animal adpressions and moulds of different size preserved in great detail and often showing organ connections. Silicified twigs and branches up to upright-standing plants, different kinds of arthropods, such as trigonotarbid and uropygid arachnids, as well as articulated skeletons of reptiles and amphibians complete the comprehensive fossil record of this diverse fossil assemblage (Rößler et al., 2009, 2012; Dunlop and Rößler, 2013; Feng et al., 2014; Spindler et al., 2017). The following pyroclastic horizon, Unit S3, represents a > 3.35-m-thick, light-red to purple-red, poorly sorted, massive, matrix-supported, unwelded coarse ash tuff with a high content of accretionary lapilli and pumice fragments. It is interpreted as deposit of a high-concentrated pyroclastic density current, entombing upright stems and hosting different size stems in horizontal position, which show alignment in the direction of the eruption centre. Among them is the largest calamite found so far (*Arthropitys bistriata*) with an estimated length of 15 m (Feng et al., 2012; Rößler et al., 2012). The lithological profile is completed by sub-recent hill-side scree, Unit S2, and a recent soil horizon, Unit S1.

Since 2009, a second excavation was established in Chemnitz-Sonnenberg covering an area of 20 × 15 m (Rößler and Merbitz, 2009), in a distance of ca. 1.5 km from the Chemnitz-Hilbersdorf excavation (Fig. 3A). The section at Chemnitz-Sonnenberg consists of three major lithological units (Fig. 3C). Unit LE1, representing the palaeosol horizon, developed on red alluvial plain deposits, but differs significantly from the palaeosol at Chemnitz-Hilbersdorf. It represents a poorly drained, fine- to medium-grained substrate that exhibits waterlogging features. The palaeosol is up to 1 m thick, shows colour changes from the red-coloured unaltered sediment to dark greyish-green and purple mottling merging into a light or intense green colour at the top, and results from clayey to silty clastic sediment. The 0.35–0.50 m thick top horizon, LE1c, is strongly lithified due to diagenetic cementation by SiO₂, originating from the overlying basal pyroclastics. At the top, LE1c bears small carbonised plant remains and vertebrate bone fragments, root moulds with clayey fill rarely occur. The overlying 0.45 m thick basal pyroclastics of Unit LE2 are characterised as purple-coloured, fine- to medium-grained and thinly bedded ash tuffs, which can be lithologically well correlated to Unit S5 at Chemnitz-Hilbersdorf excavation (Luthardt et al., 2016). The fossil record of LE2b encompasses silicified branches and leafy shoots of calamitaleans and psaroniaceous tree ferns, so far. LE2b correlates well to the major fossil-bearing deposit S5.1 at Chemnitz-Hilbersdorf. The overlying Unit LE3 represents a > 1.75-m-thick, light-purple to light-green-coloured, accretionary lapilli bearing fine- to medium-grained ash tuff, interpreted as a low-concentrated pyroclastic surge deposit. One pycnoxylic gymnosperm stem of at least 0.60 m diameter was found, so far, facing WSW direction away from the eruption centre and sunken in the basal pyroclastics of LE2 (Rößler and Merbitz, 2009).

3. Material and methods

Our data are mainly derived from collection material of the Chemnitz natural history museum. The studied specimens were collected during the last two centuries originating from the Chemnitz Fossil Lagerstätte, predominantly from the Chemnitz-Hilbersdorf site (around 50°51′58.69″ N, 12°57′32.54″ E). Some specimens originated from other localities within the same horizon, the Zeisigwald Tuff in the
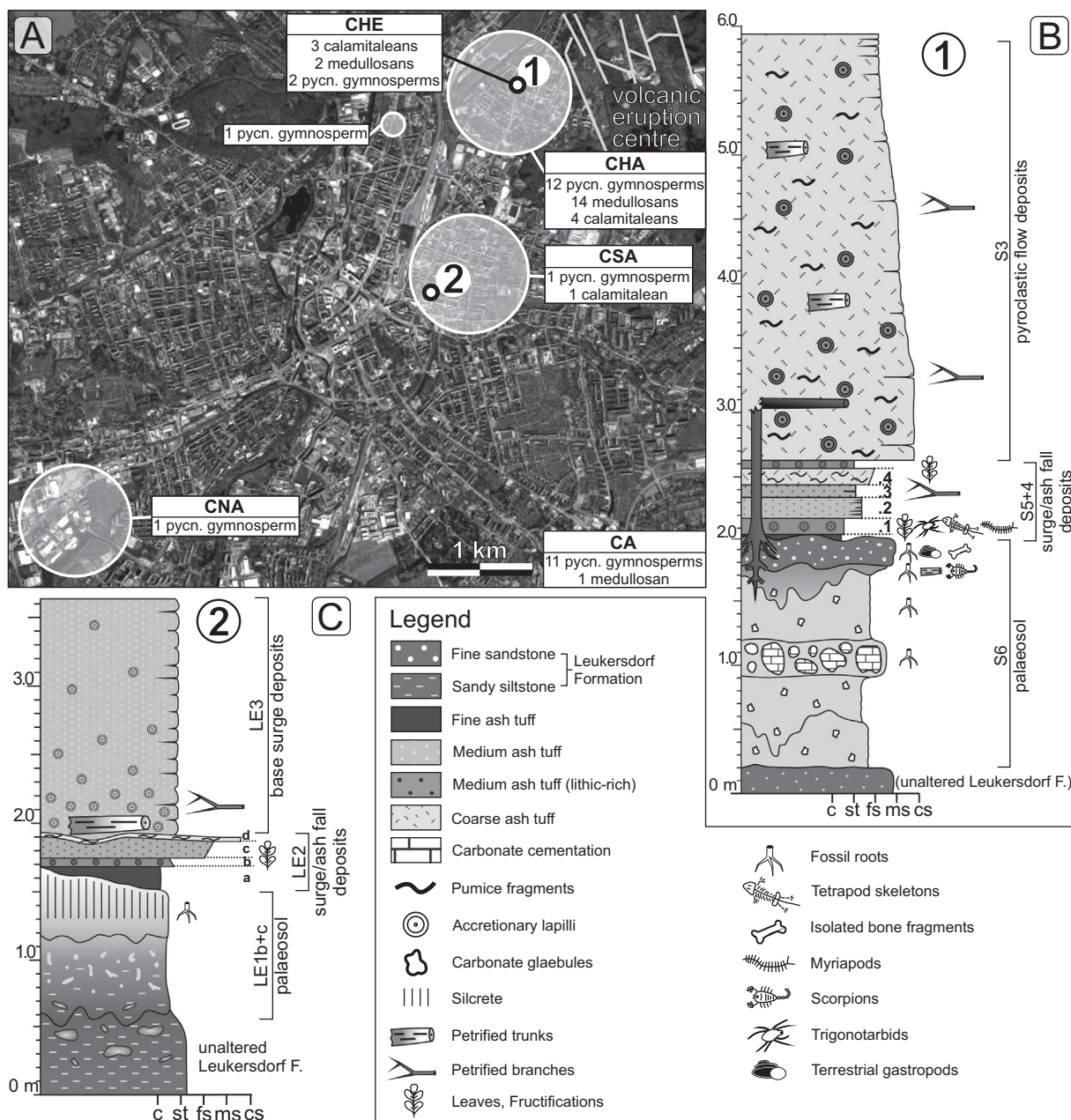
Fig. 3. (A) – Satellite image of Chemnitz showing areas where investigated specimens (*n* = 53) were found. Caldera shows eruption centre of the Zeisigwald Volcano; explanations for locality abbreviations: CA – Chemnitz area; CHA – Chemnitz-Hilbersdorf area; CSA – Chemnitz-Sonnenberg area; CNA – Chemnitz-Neefegebiet area; CHE – Chemnitz-Hilbersdorf excavation; (B) – Lithological profile of the Hilbersdorf excavation (Luthardt et al., 2016); (C) – Lithological profile of the Sonnenberg excavation (modified from Luthardt et al., 2016).

city of Chemnitz, but in some cases lacking detailed description of their location (Fig. 3A, Table 1). In addition, seven samples from the Chemnitz-Hilbersdorf excavation were investigated (compare Rößler et al., 2012). Generally, most of the specimens can be assigned to in situ upright-standing stems and short-distant transported stems or branches from the same habitat. Some of them represent stem fragments. With regard to the T^0 situation we can assume that, except from a few deadwood specimens, the majority of trees died simultaneously, which is of key importance for the correlation of tree-ring sequences.

Despite the exceptional taphonomic conditions (Rößler et al., 2012), the tree-ring record is restricted in many specimens due to imperfect preservation. Thus, only a minority of the several hundred specimens in the collection and from excavations still shows tree-ring sequences. Rarely, cell structure is adequately preserved allowing tree-rings to be characterised by cellular changes at the ring boundaries, but also by colour changes. Frequently, tree rings only remained as colour-

bands with colour changes at the ring boundaries. They are circumferential and parallel to each other, which makes them distinguishable from random colour-bands. In the majority of specimens, the extraxylary parts of the stem including cambium, cortex layers and most probably some of the outermost tree rings are missing. Definition of tree-ring terminology used in this paper is available from Supplement 3.

The 53 best-preserved specimens that were selected for tree-ring analysis (Table 1) include examples of the dominating wood producing plant groups. Among them are pycnoxylic gymnosperms, such as cordaitaleans (*Cordaixylon*, *n* = 2) and, if no clear differentiation between cordaitaleans and conifers was possible, regarded as *Agathoxylon* sp. (*n* = 26), manoxylic pteridosperms such as medullosans (*Medullosa stellata* var. *lignosa*, *n* = 17) and even sphenophytes, such as calamitaleans (*Arthropitys bistriata*, *Arthropitys sterzelii*, *Arthropitys* sp., *n* = 8). Polished transverse sections were investigated and photographed under

Table 1
Summary of important statistical results of tree-ring analysis on 53 fossil stems.

Sample no.	Species	Locality	Ring types	Stem diameter (mm)	Length of section (mm)	Number of rings	Mean ring width (mm)	Min. ring width (mm)	Max. ring width (mm)	Standard deviation	Mean sensitivity
HOG-1 seq. 1	Agathoxylon sp.	CHA	1	480 × 270	206.4	67	3.08	0.99	5.58	1.03	0.25
HOG-1 seq. 2			1		227.8	66	3.45	1.22	9.70	1.33	0.28
K133	Agathoxylon sp.	CHA	1/r?	90 × 78	32.7	15	2.18	0.82	7.69	1.73	0.32
K1177	Agathoxylon sp.	CHA	1	335 × 255	145.9	54	2.70	0.96	8.91	1.39	0.41
K1777	Agathoxylon sp.	CHA	1/3a/c	85 × 64	27.0	18	1.50	0.85	3.75	0.67	0.27
K3269	Agathoxylon sp.	CHA	1/(2)/*/r	75 × 65	38.2	7	5.46	0.58	12.26	4.37	0.70
K3367a	Agathoxylon sp.	CHA	1	Fragment	57.9	26	2.23	1.39	4.38	0.60	0.26
K3405a	Agathoxylon sp.	CHA	1/k/r	131 × 75	44.9	26	1.73	0.84	3.95	0.75	0.45
K3409	Agathoxylon sp.	CHA	1/2/*	81 × 74	38.0	18	2.11	0.71	3.32	0.77	0.32
K3503	Agathoxylon sp.	CHA	1/k/*	Fragment.	73.6	28	2.63	1.56	5.33	0.91	0.30
K3733	Agathoxylon sp.	CHA	1	Fragment.	168.5	67	2.51	1.08	4.81	0.74	0.27
K4842	Agathoxylon sp.	CHA	1/f/r	106 × 87	67.9	35	1.94	0.56	4.26	1.01	0.32
K4960 seq. 1	Agathoxylon sp.	CHA	1	280 × 160	114.6	58	1.98	0.60	4.57	0.83	0.29
K4960 seq. 2			1		123.7	58	2.13	0.78	4.12	0.85	0.27
K5358	Agathoxylon sp.	CHA	1	68 × 59	32.2	14	2.30	1.13	3.58	0.82	0.38
K3793	Agathoxylon sp.	CS	1/r?	Fragment	67.8	23	2.46	0.68	5.56	1.57	0.77
K4613	Agathoxylon sp.	CHA	1/f?/r?	222 × 114	78.0	33	2.36	1.27	4.17	0.73	0.24
K349	Agathoxylon sp.	CNA	1	Fragment.	83.2	52	1.60	0.27	3.89	0.91	0.31
K6043	Agathoxylon sp.	CA	1/(2)	221 × 205	120.4	24	5.02	0.95	12.38	3.00	0.39
K6044 seq. 1	Agathoxylon sp.	CA	1/2*	(425)	183.1	75	2.44	0.56	4.39	1.04	0.34
K6044 seq. 2			1/2*		173.7	69	2.30	0.83	0.96	2.52	0.25
K6045	Agathoxylon sp.	CA	1/(2)	275 × 269	147.0	31	4.74	1.93	12.67	3.10	0.32
K6046 seq. 1	Agathoxylon sp.	CA	1	555 × 355	227.1	70	3.20	0.93	14.94	2.14	0.29
K6046 seq. 2			1		251.7	75	3.36	1.11	6.61	1.09	0.26
K6047	Agathoxylon sp.	CA	1	140 × 110	72.4	54	1.34	0.58	2.59	0.41	0.27
K6048	Agathoxylon sp.	CA	1	275 × 183	86.8	50	1.74	0.49	5.00	0.93	0.30
K6049 seq. 1	Agathoxylon sp.	CA	1	597 × 584	236.2	64	3.69	0.99	8.82	1.67	0.36
K6049 seq. 2			1		399.0	77	5.18	0.62	11.14	2.20	0.32
K6050	Agathoxylon sp.	CA	1	256 × 152	93.3	34	2.74	1.25	5.54	1.21	0.33
K6051 seq. 1	Agathoxylon sp.	CA	1	490 × 420	238.8	53	4.50	0.95	7.59	1.60	0.28
K6051 seq. 2			1		217.6	46	4.73	0.80	10.08	2.33	0.40
K6052	Agathoxylon sp.	CA	2	Fragment.	87.4	49	1.78	0.47	4.36	0.87	0.47
KH0021-01 a	Cordaixylon sp.	CHE	1/(3?)	155 × 135	40.5	11	3.69	0.93	6.71	1.76	0.61
KH0025	Cordaixylon sp.	CHE	1/*	321 × 224	149.9	76	1.97	0.68	3.97	0.87	0.39
KH0042-03b	Arthropitys bistriata	CHE	2/3b?	215 × 162	97.6	22	4.44	1.93	7.89	1.73	0.27
KH0052-01 e	Arthropitys bistriata	CHE	2	62 × 57	20.4	13	1.57	0.44	2.26	0.53	0.37
KH0052-09 a	Arthropitys bistriata	CHE	2/k	189 × 112	71.4	26	2.75	1.39	6.81	1.26	0.44
KH0277-01	Arthropitys bistriata	CHE	2/37/k	230 × 200	63.9	19	3.36	1.09	9.92	2.43	0.45
KH0277-04	Arthropitys bistriata	CHE	2/3a/c/k/*	310 × 220	24.1	7	3.44	1.75	4.77	0.94	0.33
K3257	Arthropitys sterzelii	CHA	2/3b/k/*	139 × 126	57.9	24	2.41	0.68	5.26	1.36	0.72
K3279	Arthropitys sp.	CHA	2	Fragment.	47.9	20	2.40	0.89	4.73	1.07	0.51
K5590 a	Arthropitys bistriata	CHA	2/k	127 × 127	54.1	26	2.08	0.36	4.54	1.25	0.37
K6004 a	Arthropitys bistriata	CS	2/(1)/k/*	188 × 120	100.5	42	2.39	0.77	4.88	1.10	0.45
KH0067-02a	M. stellata var. lignosa	CHE	2/3c	136 × 110	59.2	36	1.64	0.62	6.49	1.10	0.42
KH0286-03	M. stellata var. lignosa	CHE	2/3c	89 × 62	30.8	35	1.93	0.89	6.19	1.29	0.42
K63	M. stellata var. lignosa	CHA	2	95 × 76	30.7	13	2.36	0.99	0.87	4.15	0.41
K311	M. stellata var. lignosa	CHA	2	107 × 84	23.4	12	1.95	0.65	0.75	2.84	0.47
K353	M. stellata var. lignosa	CHA	2	154 × 128	60.2	29	2.08	1.30	0.52	5.21	0.50
K621 b	M. stellata var. lignosa	CHA	2/k	330 × 260	165.8	44	3.77	0.99	16.30	2.62	0.48
K705 b	M. stellata var. lignosa	CHA	2	147 × 121	56.1	26	2.16	1.42	0.64	6.01	0.46
K2542	M. stellata var. lignosa	CHA	2	Fragment.	115.5	31	3.61	1.00	11.31	2.33	0.43
K2553	M. stellata var. lignosa	CHA	2	52 × 44	28.2	11	2.57	1.92	0.63	7.24	0.77

(continued on next page)

Table 1 (continued)

Sample no.	Species	Locality	Ring types	Stem diameter (mm)	Length of section (mm)	Number of rings	Mean ring width (mm)	Min. ring width (mm)	Max. ring width (mm)	Standard deviation	Mean sensitivity
K2579	M. stellata var. lignosa	CHA	2	Fragment.	56.1	22	1.98	1.43	0.73	7.04	0.38
K2763 a	M. stellata var. lignosa	CHA	2	81 × 77	28.7	12	2.39	0.82	0.76	4.10	0.49
K2771	M. stellata var. lignosa	CHA	2	112 × 84	52.0	16	3.25	1.16	6.98	1.75	0.49
K4013	M. stellata var. lignosa	CHA	2/3c	144 × 101	58.8	16	3.68	0.99	16.30	3.86	0.76
K4008 b	M. stellata var. lignosa	CHA	2	136 × 93	44.7	12	3.73	0.65	1.43	14.48	0.47
K4039	M. stellata var. lignosa	CHA	2	122 × 99	34.7	15	2.32	1.04	1.20	4.40	0.44
K5598	M. stellata var. lignosa	CHA	2/3c	83 × 82	26.8	12	2.34	0.83	1.30	4.03	0.31
K6042	M. stellata var. lignosa	CA	2/3c/*	257 × 162	141.2	17	8.30	2.25	29.54	7.28	0.58
Sum/average/min/max/average/average:						2081	2.81	0.27	29.54	2.32	0.41

See Fig. 4 and text for description of ring Types 1–3; See Fig. 3 for sample localities; Further phenomena in stem sections are documented by signs and lower cases: * – double or false ring; c – callus tissue; f – arthropod feeding traces; k – reaction wood or kinked rows of tracheids; r – rotten or decomposed wood. Explanations for locality shortcuts: CA – Chemnitz area; CHA – Chemnitz-Hilbersdorf area; CSA – Chemnitz-Sonnenberg area; CNA – Chemnitz-Neefegebiet area; CHE – Chemnitz-Hilbersdorf excavation.

a Nikon SMZ 1500 microscope, equipped with a Nikon DS-5 M-L1 camera. Investigated specimens are stored in the palaeontological collection of Chemnitz natural history museum (K-numbers) or in the private collection of Holger Obst, Gersdorf (HOG-1).

Cell size measurements were processed manually by microscopic camera software (NIS Elements D3.2), encompassing measurements of radial lumen diameter (RLD), radial wall thickness (RWT), lumen area (LA) and lumen circumference (LC). Lumen diameter and radial wall thickness are shown in tracheidograms (Vaganov, 1990), where radial wall thickness is presented as double radial wall thickness (DRWT), referring to the method of Mork (1928). This method defines the portion of latewood as the part of the section, where $DRWT_i \geq RLD_i$ (Denne, 1989).

Ring width data was also processed by microscope camera software (NIS Elements D 3.2). A data set of 2081 ring width measurements of 59 ring sequences from 53 specimens with 7 to 77 rings per sequence was created (Table 1).

According to Douglass (1928), mean sensitivity was determined as a measure for high variability in a ring sequence of a tree from one year to the next, delivering valuable information for palaeoecological interpretation. According to the equation of Fritts (1971), x_t marks one ring width in the whole section of n measurements in a sequence.

$$\text{Mean sensitivity (MS)} = \frac{1}{n-1} \Sigma_{t=1}^{t=n-1} \left| \frac{2(x_{t+1} - x_t)}{(x_{t+1} + x_t)} \right| \tag{1}$$

Mean sensitivity was calculated for the entirety of tree-ring sections ($n = 59$). The resulting data provide the possibility to evaluate, whether a tree is complacent or sensitive with regard to its reaction on environmental fluctuations. Following Douglass (1928), trees with values of 0.3 or lower are classified as complacent, whereas trees with mean sensitivity higher than 0.3 are classified as sensitive. Usually, mean sensitivity values are within a range of 0.0 to 0.6 (Creber, 1977). Annual sensitivity values of every neighbouring ring width couple build up a curve of a sequence, which shows trends of a tree's sensitivity during its lifetime. To point out the overall relationship of annual sensitivity and ring width, mean value curve for annual sensitivity was estimated. Values were taken from the same eleven sequences used for estimation of ring width mean value curve. These individual curves were standardised by the same procedure described and applied for ring width data.

4. Results

The existence of tree rings in arborescent woody plants from the Chemnitz Fossil Forest is clearly demonstrated. However, different morphological types of tree rings occur in the different plant groups of pycnoxylic gymnosperms, medullosan seed ferns and calamitaleans.

4.1. Tree-ring types

Combining macroscopic and microscopic observations with statistical analysis, tree rings obtained from fossil plants of different affinity were classified on the basis of their morphological properties (Fig. 4). As a result, three different tree-ring types were differentiated according to their occurrence in the investigated plant groups.

4.1.1. Type 1 – distinct tree rings

Tree rings of Type 1 are generally developed as regularly shaped, parallel and circumferential growth increments in stems and branches of pycnoxylic gymnosperms (Figs. 4, 5A). Sporadically and more irregularly they were additionally observed in calamitaleans. Type 1 rings are usually characterised by a gradual decrease of cell size and a simultaneous increase of radial wall thickness towards the ring boundary (Fig. 5B), frequently accompanied by a radial flattening of tracheids and a slightly increasing parenchyma volume (Fig. 4). After growth
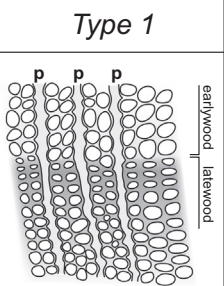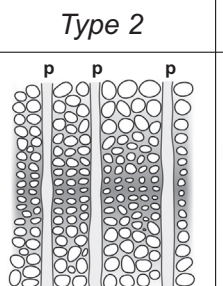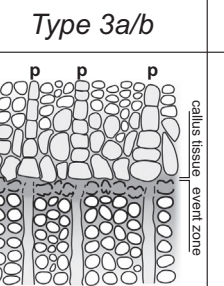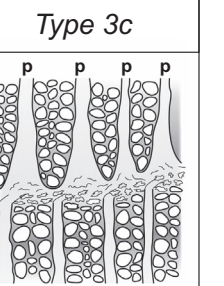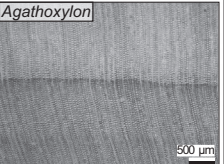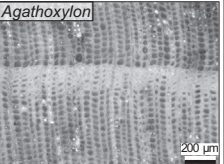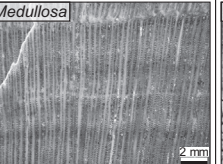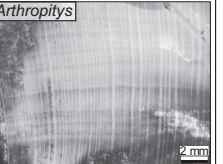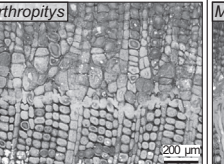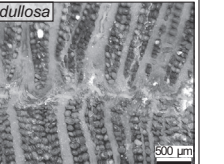
	Type 1	Type 2	Type 3a/b	Type 3c
sketch				
example	Agathoxylon (500 μm) / Agathoxylon (200 μm)	Medullosa (2 mm) / Arthropitys (2 mm)	Arthropitys (200 μm)	Medullosa (500 μm)
occurrence	distinct / regularly	indistinct / regularly	very distinct / solitary	very distinct / solitary
morphology	- distinct ring boundary - small latewood portion (according to Mork, 1928)	- diffuse ring boundary - no latewood (according to Mork, 1928)	- layer of distorted or collapsed cells - overgrown by callus tissue	- layer of distorted or collapsed cells - high parenchyma portion - rearrangement of wood structure
cells per ring	earlywood: 25-70 latewood: 2-8	30-36 (in calamitalean)	—	—
ring width	Mean: 2.78 mm Min: 0.27 mm Max: 14.94 mm	Mean: 2.78 mm Min: 0.27 mm Max: 14.94 mm	—	—
plant groups	Pycnoxylic gymnosperms	Calamitaleans Medullosans	Calamitaleans	Medullosans

Fig. 4. Overview of different ring types occurring in the investigated specimens and their morphological and statistical characteristics; p – parenchyma.

interruption, at the ring boundary initial earlywood formed with large tracheids, followed by slightly smaller tracheids, which are more or less constant in size in wide parts of the earlywood. One striking feature of Type 1 rings is the small latewood portion in comparison to the earlywood (Fig. 5C,G). Frequently, latewood and initial earlywood of Type 1 rings show crumpled cells and bent or buckled radial columns of tracheids (see Supplement 2 for more detailed description).

K3409, a pycnoxylic gymnosperm (*Agathoxylon* sp.) from Chemnitz-Hilbersdorf, measures 81×74 mm in diameter and possesses well preserved tree rings down to cell level (Fig. 5A). From the presence of reaction wood due to mechanical stress, the low number of 18 recorded rings and generally smaller cells than in K6044, K3409 seems to represent the branch of a tree. Cell size parameters were measured in a section of four Type 1 rings and possibly intercalated intra-annual rings or false rings in the inner part of the branch section. Cell size development in the measured sections shows clear changes of radial lumen diameter and radial wall thickness at the ring boundaries (Fig. 5E–G). The mean radial lumen diameter is 28 μm, but reaches up to 39 μm in the earlywood and down to 12 μm in the latewood. Lumen area varies from 690 to 750 μm^2 in the initial earlywood, from 270 to 620 μm^2 in the older earlywood and decreases down to 125 μm^2 in the latewood. Both lumen area and radial lumen diameter decrease significantly close to the ring boundary, representing the latewood portion. In contrast,

radial wall thickness increases towards the ring boundary. The tracheidogram (Fig. 5F) shows that double radial wall thickness exceeds the lumen diameter in 2 to 8 consecutive rows of tracheids. The earlywood encompasses 25–70 rows of tracheids. Of the three measured rings, the latewood portion varies between 7.5 and 13.5%, with a mean value of 10.6%. Several cells on the verge of the earlywood-latewood boundary, lumen diameters already decrease dramatically and characterise this part as "transition zone" (Fig. 5G). In general, cell sizes show a high variability, especially in the earlywood. While radial wall thickness increases steadily, lumen diameter stays more or less constant in the earlywood before it decreases in the transition zone. Radial wall thickness does not exceed lumen diameter in the growth interruptions F-3a and F-3b, but for one cell in F-2 (Fig. 5F). These interruptions most likely represent false rings or intra-annual rings.

K6044, the segment of a large pycnoxylic gymnosperm trunk (*Agathoxylon* sp.) exhibits a radial diameter of up to 425 mm and a record of 75 tree rings (Supplement 4). Cell size parameters were measured in a section of seven tree rings in the innermost part of the stem, a zone of high preservational detail. Lumen area of initial earlywood is 1900–2500 μm^2, of later earlywood around 1300 μm^2 and of latewood 130–550 μm^2. The latewood portion is somewhat higher compared to K3409 with 7 to 19 versus 14 to 44 rows of tracheids in the earlywood.
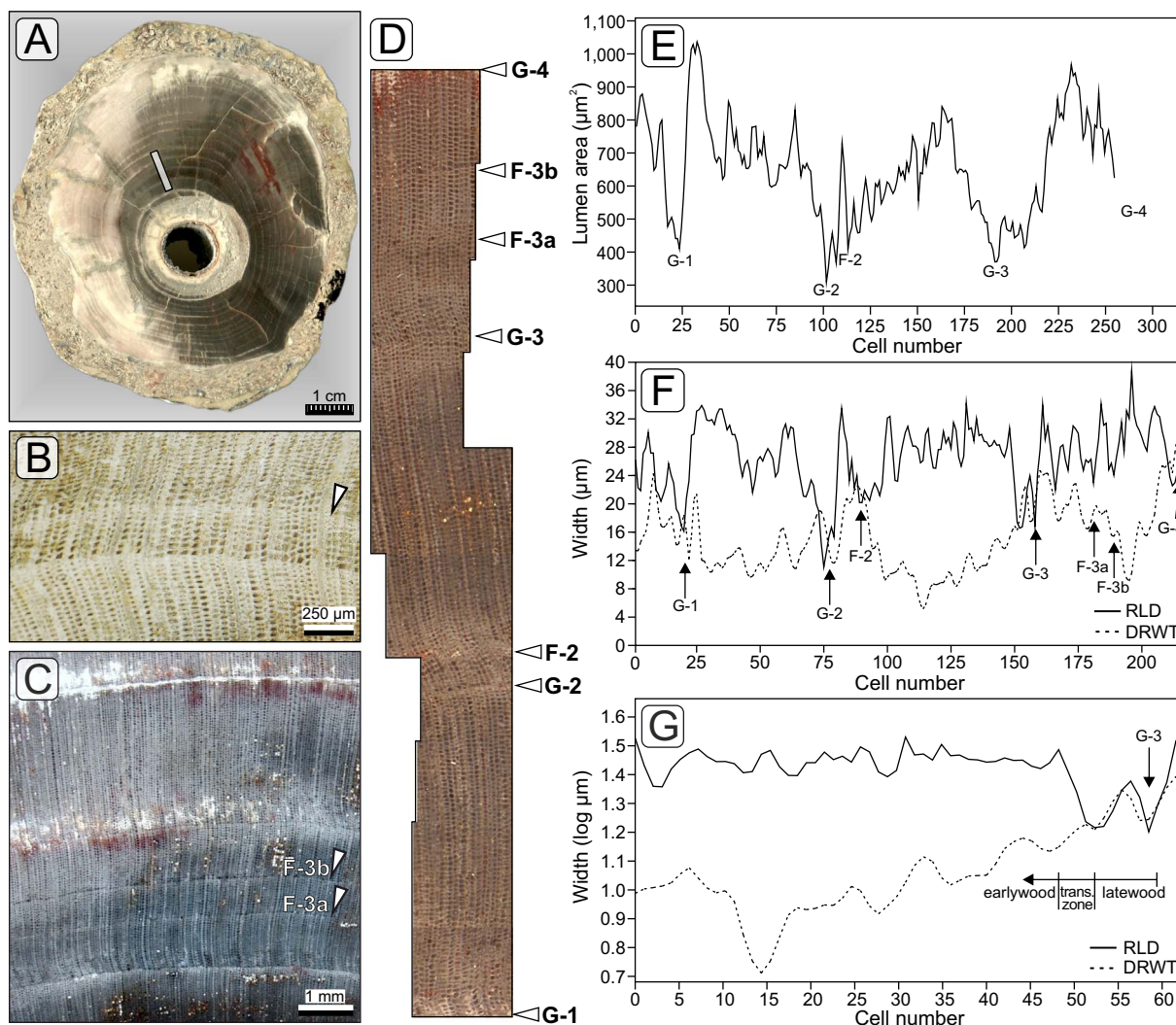
Fig. 5. Characterisation of Type 1 regular tree rings and cell size measurements on K3409 (*Agathoxylon* sp., Chemnitz-Hilbersdorf area). (A) Section of K3409 showing well preserved tree rings; white rectangle shows measured section in D–G; (B) – Tree ring followed by a false ring (arrow) in the initial earlywood in K3409; (C) – Less distinct false rings F-3a and b in polished section of K3409; (D) – Sequence of cell size measurements showing tree rings G-1 to 4 and false rings F-1 to 3; (E–G) – Cell size parameters of measured section in (D) with marked tree-ring/false-ring boundaries shown as smoothed mean curves. RLD – Radial lumen diameter, DRWT – double radial wall thickness. Classification of late- and earlywood in (G) corresponding to Mork (1928).

4.1.2. Type 2 – indistinct tree rings

Tree rings of this type usually occur in calamitaleans and me-dullosans as regular, mostly circumferential, but more indistinct zones. They are defined by a gradual decrease of cell size towards latewood, followed by a gradual increase of cell size in the transition to earlywood so that no clear ring boundary is visible (Figs. 4,6B). The occurrence varies from very distinct to nearly invisible; occasionally, rings show a similar morphology as Type 1 rings. As a result of taphonomic pro-cesses, compaction and even destruction of cells can appear in the zone of highest density; this is most frequently observed in calamitaleans.

KH0277-01, a slice from the middle stem part of a tall calamitalean (*Arthropitys bistriata*), was found in growth position at Chemnitz-Hilbersdorf (Rößler et al., 2014, p. 76, pl. 2) and measures 212 × 190 mm in diameter. A section of four consecutive rings was captured from the outer part of the stem (Fig. 6A). Ring boundaries are macroscopically indistinct. In the tracheidogram (Fig. 6D), they are traceable by a successive decrease of lumen diameter and lumen area, as well as a concurrent increase of radial wall thickness. Changes of lumen diameter range between 43 and 68 μm on average, and changes of radial wall thickness range between 10 and 26 μm on average, whereas double radial wall thickness does not exceed the lumen dia-meter. Ring boundaries are characterised by smaller tracheids and

thicker tracheid walls by trend. As in the case of ring boundary G-3 (see Fig. 6D), changes in cell size parameters are sometimes not even sig-nificant enough to set apart from the "noise" of normal fluctuations. Between ring boundaries of G-1 and G-2, a potential false ring (F-1) occurs, indicated by smaller cells and increased radial wall thickness, which is, however, macroscopically invisible (Fig. 6D).

4.1.3. Type 3 – event rings

In contrast to Type 1 and Type 2 rings, Type 3 rings do not occur regularly but are solitary in a stem section and can be described as event rings (Fig. 4). They were observed in calamitaleans and me-dullosan seed ferns, but only in one pycnoxylic gymnosperm. According to their anatomical characteristics, three sub-types a–c can be dis-tinguished.

Type 3a rings represent zones of injured living wood tissue, which are overgrown by parenchymatous tissue forming callus (Fig. 7B). An event ring of this type was observed in a pycnoxylic gymnosperm (K1777; Fig. 7E) and the calamitalean KH0277-04 (*A. bistriata*; Fig. 7A–D). In KH0277-04, the event ring extends over 75% of the whole stem circumference and is characterised by a sharp transition from normal wood tissue to a row of crushed tracheids (Fig. 7C,D). Normal growth of tracheids sets in again by the formation of wide
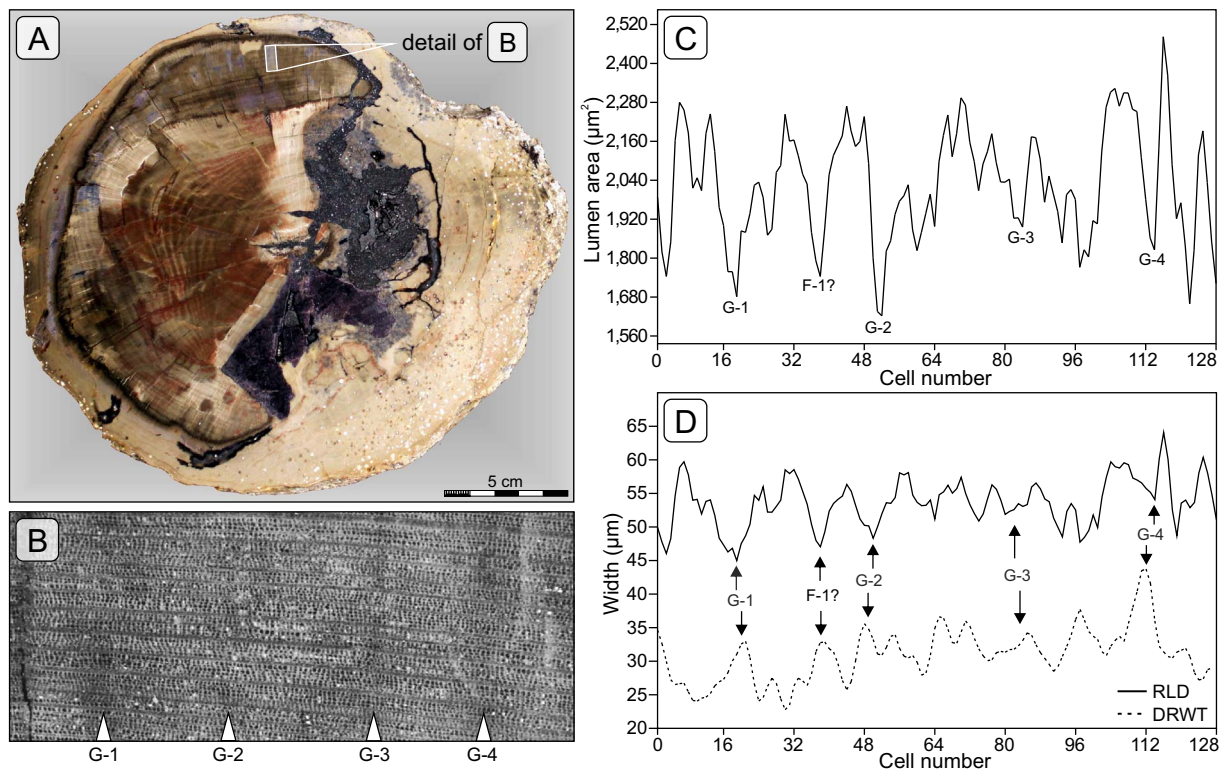
Fig. 6. Characterisation of Type 2 growth increments and cell size measurements on specimen KH0277-01 (*Arthropitys bistriata*, Chemnitz-Hilbersdorf excavation). (A) – Polished section of the middle stem section of the upright-standing calamitalean KH0277 showing areas of different preservation quality; (B) – Measured section of regularly occurring growth increments G-1 to G-4 in the outer part of the stem visible as indistinct shaded lines; (C–D) – Cell size parameters of measured section in (B) shown as smoothed mean curves. Growth increments show no latewood portion according to Mork (1928) in (D).

lumen tracheids (Fig. 7C). Callus tissue has overgrown the wounded area from both sides (Fig. 7B).

Type 3b is also not circumferential. It occurs in calamitaleans, e.g. in K3257 (*Arthropitys sterzelii*), representing a 139 × 126 mm diameter stem, found in Chemnitz-Hilbersdorf (Rößler and Noll, 2010, pl. VIII, 1, 5). The event ring is associated with a distinct tree ring in the outer part of the stem showing a gradual thickening of tracheid walls towards the ring boundary. At the ring boundary, tracheids of one row are damaged by disruption (Fig. 7F), followed by initial growth of up to four rows of large, thin-walled parenchymatous cells. The latter gradually decrease to normal size in the further growth continuation and growth of normal tracheids sets in again.

Type 3c is, in contrast to Types 3a/b event rings, mostly circumferential and specific to medullosans (Fig. 7G–L). In contrast to normal Type 2 rings in medullosans the event rings indicate a striking growth interruption. In front of the ring boundary, usual changes of tracheid size parameters, such as tracheid wall thickness or decrease of lumen width are not clearly recognisable. At the ring boundary, tracheids are frequently distorted, which is most probably not taphonomically induced because surrounding cells remained intact (Fig. 7H,I). The zone of distorted tracheids is overgrown by undifferentiated parenchyma, forming a circumferential parenchyma band (Fig. 7L). Initial growth after the ring boundary is characterised by reorganisation of the arrangement of tracheids and rays (Fig. 7I). In the sections of investigated medullosan specimens, up to four consecutive Type 3c event rings can be recognised. In five of seventeen medullosans one or two event rings appear in the outermost part of the transverse section, followed by an exceptionally wide tree ring (Fig. 7J). However, it is possible to correlate this ring among the investigated specimens that all originate from Chemnitz-Hilbersdorf. Two of them were found in growth position at the Chemnitz-Hilbersdorf excavation (KH0067-02a, KH0286-03).

4.1.4. False rings

Associated with regular Type 1 and Type 2 tree rings, further growth phenomena occur. Irregular intra-annual rings or false rings can be distinguished from regular tree rings in several cases. Frequently, these false rings follow a regular tree ring by a short distance of 100–300 μm, are less distinctly developed and can fade out laterally (Fig. 5B). Sporadically, up to two of these false rings are present within a regular tree ring (Fig. 5C). Their position within increments of regular rings shows no clear trend to occur preferred in early- or latewood. Morphologically, they are more similar to Type 2 rings. Thus, false rings could be distinguished from normal rings in pycnoxylic gymnosperms, but in calamitaleans and medullosans the identification of false rings remains problematic.

4.2. Ring width data and mean sensitivity

Individual ring sequences were evaluated by comparing them (1) within single specimens, (2) among different specimens of the same plant group and (3) among all investigated specimens within the former habitat (Table 1). Total mean ring width (MW_T) was calculated from all ring sequences ($n = 59$) providing a value of $MW_T = 2.81$ mm, whereas the smallest value of MW = 1.34 mm was calculated for K6047 (*Agathoxylon* sp.) and the largest value of MW = 8.30 mm for K6042 (*Medullosa stellata* var. *lignosa*). Variation of mean ring width between different plant groups is comparatively low (Fig. 8A,C). Pycnoxylic gymnosperms and calamitaleans show nearly the same average mean ring width of MW = 2.78 and MW = 2.60 mm, whereas medullosans show a slightly higher value of MW = 2.94 mm accompanied by a higher standard deviation due to specimen K6042 representing a statistical outlier. In several medullosans (e.g. K6042, K621b) single ring widths of up to 29.54 mm were measured, being nearly five times higher than mean values of the according sections. Calamitaleans show the smallest variability in mean ring width among the specimens.
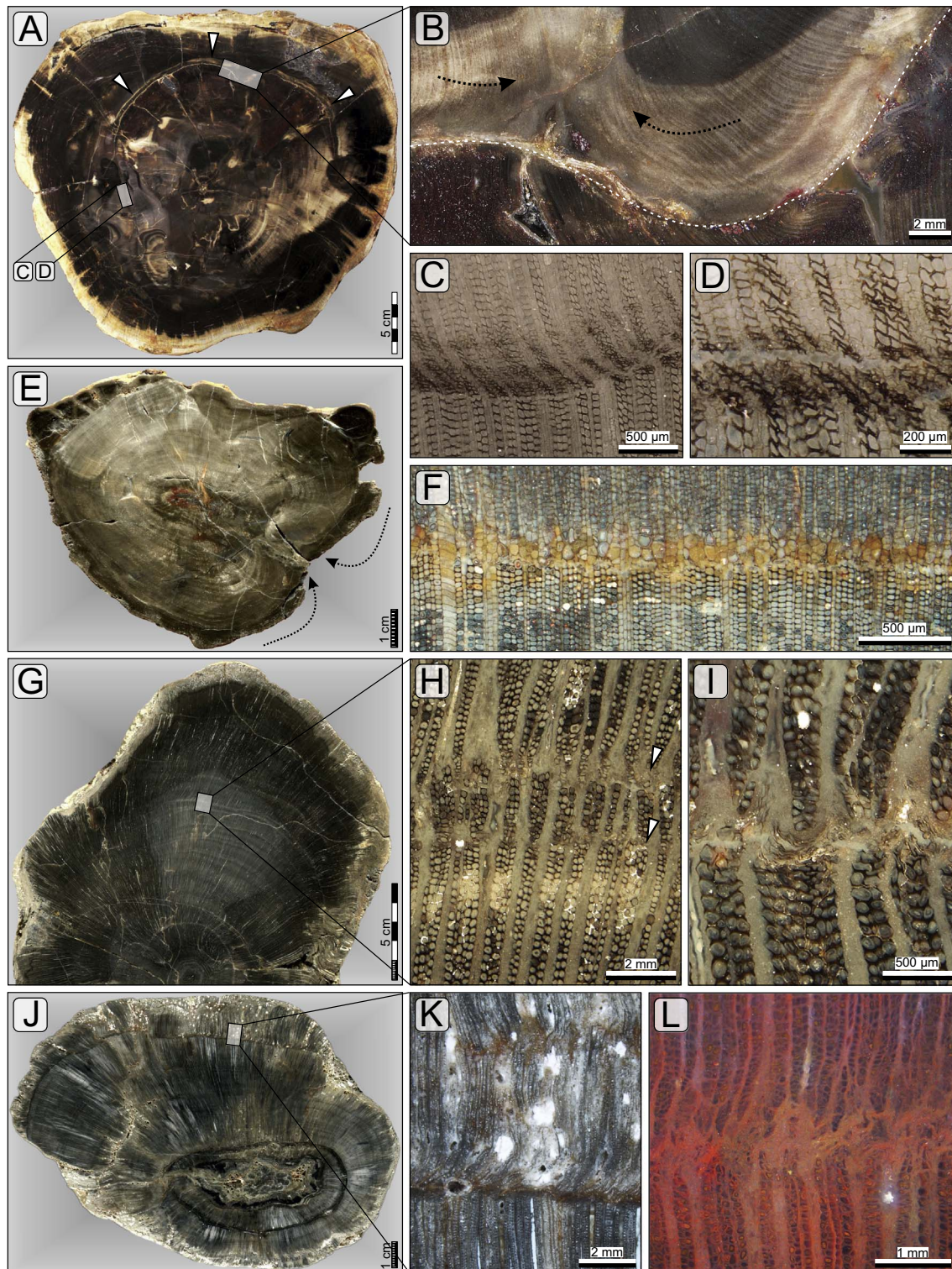
Fig. 7. Occurrence of Type 3a–c rings in polished sections of selected specimens. (A) – Distinct event ring of Type 3a (arrows) in polished section of KH0277-04 (*A. bistriata*; Chemnitz-Hilbersdorf excavation) indicating severe injury, which was overgrown by callus tissue shown in (B), whereas arrows in (B) indicate growth directions from both sides. White dashed line marks tissue boundary of the injury; (C) – Detail of the same event ring with small thick-walled cells in the following, instead of callus tissue; (D) – Detail close to section of (C), showing crushed and distorted cells in the event ring; (E) – Injury zone overgrown by callus tissue in K1777 (*Agathoxylon* sp.) similar to (A) but without distinct event ring; (F) – Event ring of Type 3b in calamitalean K3257 (*A. bistriata*) showing a row of distorted cells overgrown by large initial parenchyma cells; (G) – Polished section of K6042 (*Medullosa stellata* var. *lignosa*) with regular "type 2" growth increments and Type 3c event rings; (H) – Detail of two event rings in (G), see arrows. Event rings show growth interruptions by deformed cells and an initial reorganisation of parenchyma bands; (I) – Detail of an event ring in K38 (*Medullosa stellata* var. *lignosa*) showing crushed and distorted cells at the ring boundary and increased initial parenchyma formation; (J) – Regular Type 2 growth increments and distinct Type 3c event ring in the outer part of the stem of K4013 (*Medullosa stellata* var. *lignosa*), as it is frequently observed in further medullosans; (K) – Detail of (J) showing growth interruption; (L) – Distinct Type 3c event ring in the marginal stem part of K2642 (*Medullosa stellata* var. *lignosa*) indicated by a circumferential parenchyma band.
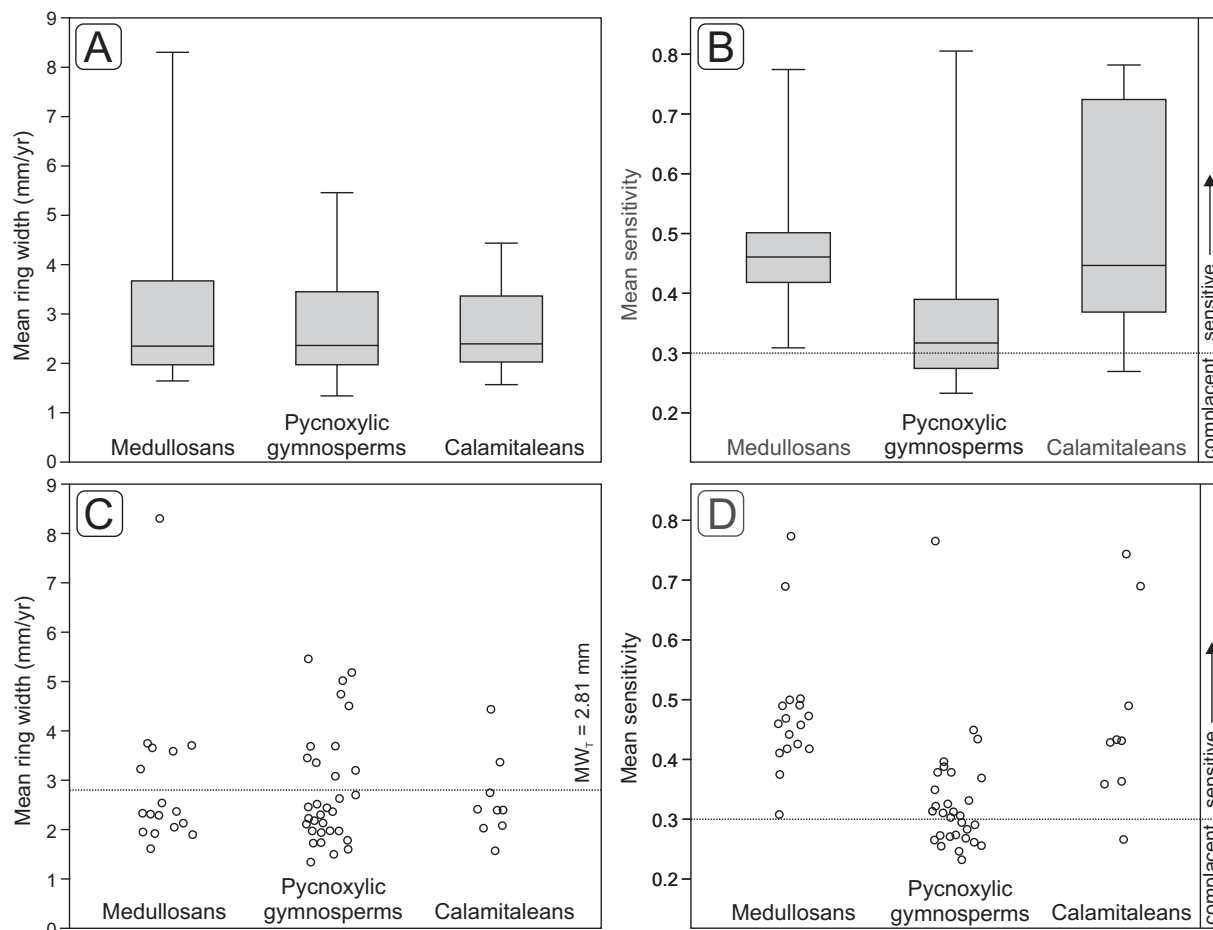
Fig. 8. Statistical analyses of mean ring width (A,C) and mean sensitivity (B,D) from the entirety of specimens, comparing the three major plant groups of medullosans ($n = 17$), pycnoxylic gymnosperms ($n = 28$) and calamitaleans ($n = 8$). Results presented as boxplot (A,B) and jitter plot diagrams (C,D). MWT in (C): mean ring width of all specimens.

Smallest ring width of all specimens was 0.27 mm measured in the pycnoxylic gymnosperm K349.

Mean sensitivity was calculated for every ring sequence being representative for average values of the different plant groups as well as for the entirety of investigated specimens. The overall mean sensitivity (MS_T) of all specimens is $MS_T = 0.41$ ($n = 59$). In contrast to mean ring width, mean sensitivity values show a higher variability by comparing them between different plant groups (Fig. 8B,D). Medullosans have the highest average mean sensitivity of $MS = 0.48$, which classifies them as sensitive according to Douglass (1928). Values of individual ring sequences range between $MS_{max} = 0.31$ and $MS_{min} = 0.77$ attributing obvious sensitivity to all specimens. For calamitaleans, a mean sensitivity of $MS = 0.44$ was calculated, demosntrating that they were slightly more sensitive as medullosans. Mean sensitivity of individual ring sequences show a high variability in a range of $MS_{max} = 0.27$ (complacent) and $MS_{min} = 0.72$ (strongly sensitive). In contrast, pycnoxylic gymnosperms show on average lower sensitivity than both medullosans and calamitaleans do; a value of $MS = 0.35$, which is, however, still regarded as sensitive. Moreover, gymnosperms show a smaller variability among individual specimens within the 25–75 percentiles. Single outliers reach a minimum value of $MS_{min} = 0.24$, which is complacent, and maximum values of $MS_{max} = 0.77$, which is strongly sensitive and represents the highest value among all investigated specimens.

With regard to the number of investigated specimens, calculated values for pycnoxylic gymnosperms exhibit the highest statistical significance. However, variation of mean sensitivity of different ring sequences in the same stem section of a specimen can be significant. In K6044, two sequences were measured providing values of $MS_1 = 0.34$

(sensitive) and $MS_2 = 0.25$ (complacent). A few ring sequences of pycnoxylic gymnosperms show a typical trend of slightly decreasing growth rates with ageing of the tree, which is apparent in K6044 (see Supplement 4). Annual sensitivity was slightly higher during the juvenile stage of the plants and decreased with increasing age, which is in accordance to previous studies (e.g. Creber and Chaloner, 1984).

Successively accumulating radius of stems with proceeding number of tree rings reflects a plant's growth rate, and thus its wood production (Worbes et al., 2003; Mbow et al., 2013; Fig. 9). Pycnoxylic gymnosperms show linear growth rates during their lifetime, whereas the estimated mean linear regression has a slope factor of $a = 3.16$ (Fig. 9A).

Most medullosans neither show a trend of decreasing growth rates with ageing nor a clear decrease of annual sensitivity, although ring sequences were up to 44 increments long. Growth rates during lifetime of individuals vary in most cases from the ideal linear trend (Fig. 9B). In the exceptional case of specimen K621b (*Medullosa stellata* var. *lignosa*), a trend of decreasing annual sensitivity with ageing, but not of growth reduction is observed. Generally, medullosans show a lower average wood production rate compared to pycnoxylic gymnosperms, expressed by a slope parameter of $a = 2.57$ of the mean linear regression curve (Fig. 9B). Many medullosans show 1 to 3 very wide tree rings in the outermost part of the sections of up to 17 mm.

Growth trends of calamitaleans are similar to those recognised in pycnoxylic gymnosperms, although not all of them show such a clear reduction of growth rates with ageing. Nevertheless, most of the specimens exhibit a clear trend of decreasing annual sensitivity and linear growth trends. The estimated slope parameter of the mean linear regression curve is $a = 2.75$ pointing to generally low growth rates similar to medullosans (Fig. 9C).
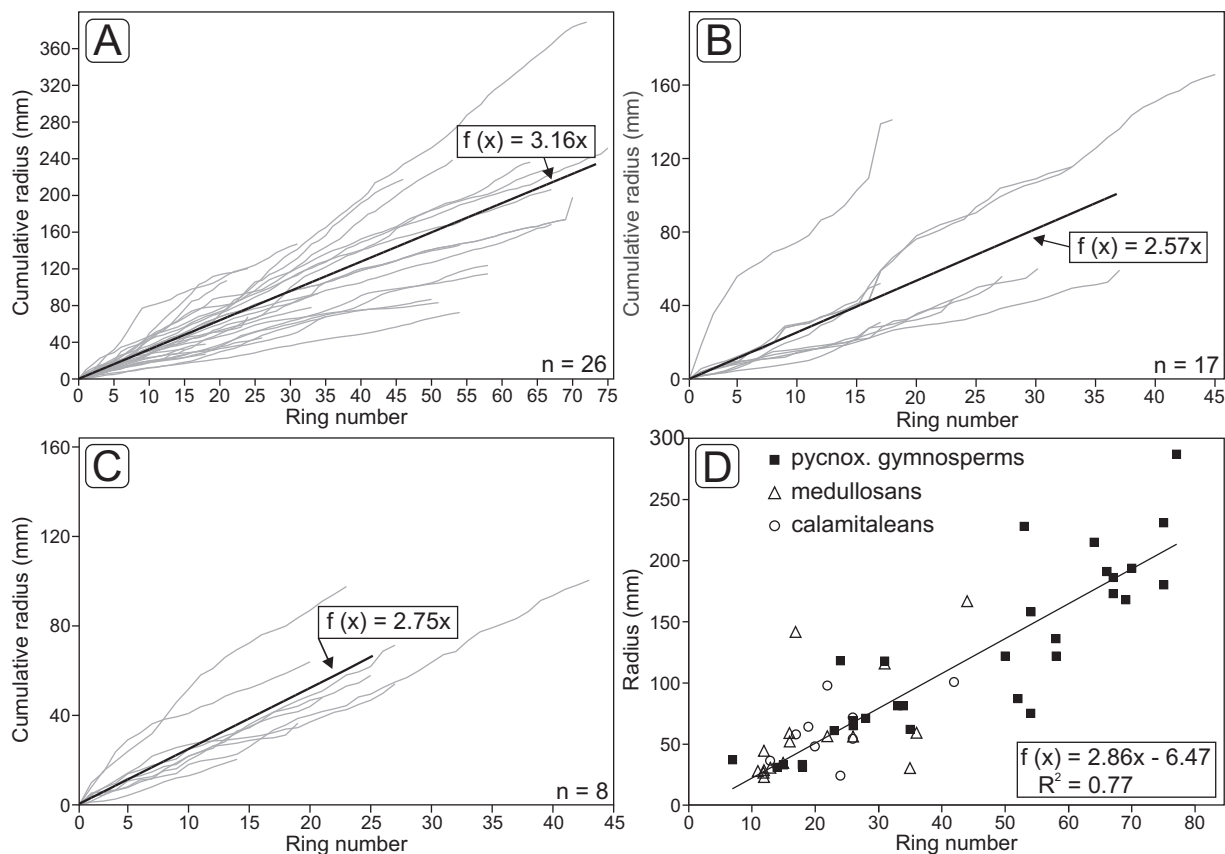
Fig. 9. Growth statistics as a measure of wood production based on ring width measurements of all investigated specimens. Diagrams show annual growth rates of individuals throughout their lifetime (grey lines) and estimated growth function of mean values (black line, formula) of the corresponding plant group. Slope factor of the function is a measure of wood production rate. (A) – Growth patterns of pycnoxylic gymnosperms; (B) – Growth pattern of medullosans; (C) – Growth patterns of calamitaleans; (D) – Statistical correlation of stem radius and the number of counted rings; linear regression (black line) was estimated for pycnoxylic gymnosperms showing a statistically robust correlation between both parameters; function could be used to estimate age of pycnoxylic gymnosperms based on their stem radius.

Correlation between the radius of the stems and the number of counted tree rings is shown in Fig. 9D. Equation of the linear regression is a function of secondary growth rate of the entirety of investigated specimens with increasing age.

5. Discussion

Tree rings in arborescent plants from the Chemnitz Fossil Forest were already shown in calamitaleans (Rößler, 2006; Rößler and Noll, 2010), but without quantitative evaluation. The comparably large amount of data collected for the present study offers the opportunity to quantify palaeoecological adaptions of the different plant groups and discuss their physiological adaptations to the palaeo-environment, extending over a tree-ring record of ca. 80 years (Luthardt and Rößler, 2017). Due to the taphonomic restrictions, the available fossil tree-ring data do not completely comply with criteria of modern dendrochronological studies (Cook and Kairiukstis, 1990), but come close to it.

5.1. Formation of tree rings and palaeo-environmental implications

The formation of regular tree rings in woody trees of the Chemnitz Fossil Forest occurs as a plant's reaction to seasonal environmental fluctuations. Major limiting factors for tree growth and thus the formation of seasonal tree rings are temperature, light, water supply and floods (Worbes, 1985; Schweingruber et al., 2006). As it was shown by sedimentological and mineralogical approaches, palaeoclimate of the Chemnitz forest ecosystem was strongly seasonal, characterised by an alternation of distinct dry and wet phases (Luthardt et al., 2016).

Therefore, it appears most likely that the major limiting factor to plant growth was water supply, leading to different patterns of growth interruptions or inhibition during dry seasons. In modern gymnosperms, water stress has in fact a direct influence on cell numbers, cell size and radial wall thickness (Zahner, 1963), and thus on the percentage of latewood (Creber and Chaloner, 1984), usually causing an abrupt transition from earlywood to latewood (Harris, 1955). Hence, formation of small latewood portions of Type 1 rings can be regarded as a reaction to water deficiency. Following Fritts (1971), small but distinct latewood portions are typical for tree rings formed under severe droughts (Fig. 5G). As Type 2 rings are morphologically similar to drought-induced false rings in modern gymnosperms, their regular occurrence in calamitaleans and medullosans further supports their formation during seasonal dry phases (compare to Glock and Aegerter, 1962).

The palaeosol at Chemnitz-Hilbersdorf excavation shows good drainage properties suggesting that water storage potential was low. From the occurrence of carbonate nodules it can be supposed that evaporation was high during dry periods causing a loss of water in the densely rooted upper palaeosol horizon by a falling groundwater table (Luthardt et al., 2016). This probably had a direct effect on smaller shallow rooting plants, such as many of the medullosans, whereas cordaitaleans and tall calamitaleans as deep rooting plants still had access to the groundwater resources (Luthardt et al., 2016). In contrast, the clayey palaeosol at Chemnitz-Sonnenberg excavation shows properties of substrate waterlogging and higher water storage potential. To what extent the heterogeneity of site-specific conditions in the whole forest ecosystem influenced tree growth and tree-ring formation still remains open, because material from other fossil sites than Chemnitz-
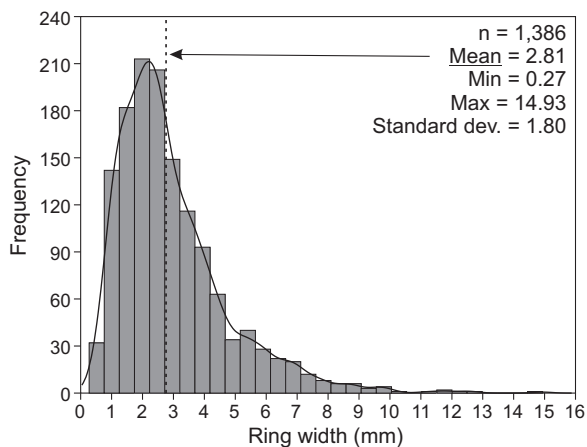
Fig. 10. Histogram plot showing size distribution of all measured pycnoxylic gymnosperms Type 1 tree rings. Size class bars show a right-skewed normal distribution, whereas majority of ring width values are in between one and four millimetres.

Hilbersdorf are so far under-represented (Fig. 3A, Table 1).

The entire mean sensitivity of all investigated specimens ($MS_T = 0.41$) is > 0.3 suggesting that plants were sensitive on average. After Schweingruber (1996) sensitivity represents a species-specific expression of the degree to which a plant reacts to environmental factors. Thus, high MS_T gives only a rough estimate that plants grew under more or less unfavourable environmental conditions, whereas climate and soil properties are regarded as major influencing factors (Douglass, 1928; Fritts, 1971; Creber, 1977). Douglass (1928) defined three types of mean sensitivity for modern trees in relation to soil moisture whereas trees of swampy basins show low mean sensitivity and on dry climate soils high mean sensitivity. The average mean sensitivity of the Chemnitz pycnoxylic gymnosperms (MS = 0.35) is similar to the intermediate type of 'Moist upland' (MS = 0.33), which is characterised by a limited water supply. This comparison shows that ring width variations in the investigated specimens were triggered by water availability during the wet season. Referring to Type 3 event rings and increased mean sensitivity, it is assumed that drought periods were generally prolonged and sometimes severe, causing plant physiologic stress. Initial calcrete formation in the upper Leukersdorf Fm. of the Chemnitz Basin (Schneider et al., 2012) suggests several months of drought season (> 6 months of evapotranspiration > precipitation, after Buol et al., 1997).

Comparable tree-ring data from the Permian are rare, but available from the Northern Tocantins Petrified Forest in Brazil (Benício et al., 2015), where a mean ring width of $MW_T = 3.49$ mm and an average mean sensitivity of MS = 0.78 was calculated from 32 measured gymnosperms (Benício et al., 2015). Whereas growth rate in Tocantins gymnosperms is only slightly higher compared to gymnosperms from Chemnitz (MW = 2.84 mm), average mean sensitivity is significantly higher as of the Chemnitz gymnosperms (MS = 0.35) suggesting different growth conditions in both ecosystems referred to physiologic stress. In fact, the Tocantins Petrified Forest tends to once have grown under relatively dry and pronounced seasonal palaeoclimate in a high-energetic sedimentary environment (Lima Filho, 1999; Rößler, 2006). This is indicated by well-drained fluvial deposits of ephemeral river systems (e.g. Rößler, 2006), massive gypsum horizons in the upper Motuca Fm. (Dias-Brito et al., 2007), and the occurrence of xeromorphic tree ferns (Tavares et al., 2014). Thus, average mean sensitivity in gymnosperms from both study sites could mirror differences of environment-induced physiological stress in the habitats, although species-specific variations cannot be excluded. Unfortunately, the Tocantins fossil localities do not represent a T^0 assemblage and reliable stratigraphic position is still unclear (e.g. Rößler et al., 2014; Neregato et al., 2017), which restricts more detailed comparability of tree-ring

data with the Chemnitz Fossil Forest.

5.2. Annual character of tree rings

To use tree rings for age determination or to acquire growth rate estimations of trees, their annual character has to be evaluated. Growth rings in its narrow sense (Creber, 1977) are restricted by definition to trees of middle to high latitudes, being formed by annually alternating differences in day length or solar radiation, respectively. In equatorial regions, however, solar radiation is more or less constant so that formation of growth rings in both modern and fossil trees was neglected for a long time. Nevertheless, there is a growing awareness that we are faced with tree-ring-like patterns in tropical Pangaea (Falcon-Lang, 1999; Benício et al., 2015) and in modern tropical environments (Worbes, 2002; Rozendaal and Zuidema, 2011). In the modern tropical realm, seasonal fluctuations in precipitation rates are induced by shifts of the Inter-Tropical Convergence Zone (ITCZ) causing alternating wet and dry seasons. In monsoonal regions, however, two or more distinct annual growth seasons could appear, prompting the formation of up to four tree rings per year in woody trees (Ash, 1983). Tree-ring characteristics developed under monsoonal climate with more than one annual growth season are described from modern wood by Ash (1985) and from pycnoxylic gymnosperm wood from the Mississippian by Falcon-Lang (1999). According to these studies, tree rings induced by monsoonal climate with multiple growth seasons per year are more or less indistinct, discontinuous in transverse sections, possess generally low mean ring widths (0.83 mm in Falcon-Lang, 1999) and high ring width variation resulting in more than one size class reflected by multi-peaked asymmetrical distribution in histograms. Regular tree rings of pycnoxylic gymnosperms in this study show distinct, continuous rings with a mean ring width of MW = 2.78 mm, varying from 0.27–14.93 mm among the mean values of 32 measured ring sequences (Table 1). In contrast to tree-ring characteristics in Falcon-Lang (1999), histogram plot shows a normal distribution giving evidence of one single size class (Fig. 10) that indicates regular growth seasons of similar duration.

The British Isles were holding a palaeolatitude of 4° S during the early Carboniferous (Falcon-Lang, 1999), and were thus continuously located in the area of ITCZ influence suggesting very high precipitation rates and indistinct, irregularly occurring seasons. The Chemnitz Fossil Lagerstätte, in contrast, was located at ca. 15° N and influenced by the Permotriassic super monsoon system, which developed as a result of the Pangaea supercontinent configuration (Parrish and Peterson, 1988). Palaeoclimate of early Permian southern and central Europe was characterised by increasingly drier conditions and strong monsoonal seasonality (Tabor and Montañez, 2004; Schneider et al., 2006; Roscher et al., 2011). Consequently, palaeoclimatic conditions of early Permian Central Europe and early Carboniferous British Isles (Falcon-Lang, 1999), under which tree rings were formed, differ significantly. The same counts for modern climatic conditions of the locality in north-eastern Australia (Ash, 1985), which is located in a near-coastal position with high precipitation rates and less distinct seasons and thus not comparable to Permian climate and Pangaea continent configuration.

Finally, it can be concluded that regular tree rings in woody plants from the Chemnitz Fossil Forest most likely reflect true annual rings, which were formed under subtropical, strongly seasonal climate. Nevertheless, intra-annual rings occur occasionally as a result of intra-seasonal fluctuations of either drought in the wet season or a pluvial event during the dry season leading to a short-time reactivation of the cambium. Even a single three-week-drought can cause the formation of a false ring in modern gymnosperms (Larson, 1963). The repeatedly observed occurrence of double rings refers to small-scale fluctuations in the season's transition either from wet to dry season or vice versa.

5.3. The significance of event rings (Type 3)

Event rings of Type 3 were investigated with regard to their environmental significance and correlation potential among the trees in the forest habitat, especially within the restricted Chemnitz-Hilbersdorf site. Different kinds of exceptional distinct growth interruptions are documented with this study (Fig. 7). By reflecting zones of destroyed outer living cells in medullosans and calamitaleans occasionally overgrown by callus tissue, these event rings are the result of severe environmental impact on plants, either caused by a superordinate event affecting the majority of the living plant community or accidental events on individuals. Studies on modern living trees showed that severe droughts, frost events in the growing season, wildfires, fungi or insect attacks could result in event rings within individuals of a whole community (Schweingruber, 2001; Schweingruber et al., 2006; Byers et al., 2014). After correlating ring sequences of predominantly medullosans and one calamitalean, an accumulation of Type 3b/c event rings is observed in the outer part of the stems, a few years before the T⁰ burial of the forest ecosystem. Causes of these growth interruptions seem to have influenced medullosans and some calamitaleans, but no pycnoxylic gymnosperms. Distortion or collapse of living cells usually results from exceptionally high or low turgor during severe events as wild fire, lightning strike, frost or droughts (Schweingruber, 2001). Type 3b/c revent rings (Fig. 7F,I) are anatomically similar to frost rings in conifers of the temperate zone (Creber and Chaloner, 1984). However, severe frost events are regarded as unlikely for the investigated Chemnitz Basin, although the Gondwana glaciation reached its maximum (e.g. Angiolini et al., 2009). Severe droughts may also cause frost-ring like damage to living tissue, as the formation process is very similar (Barnett, 1976; Schweingruber, 2001). False rings found in pycnoxylic gymnosperms support the existence of intra-seasonal droughts, which could have had stronger impact on the more sensitive medullosans and calamitaleans. Although we cannot finally exclude alternative causes mentioned above, we tend to interpret Type 3b/c event rings as drought-induced.

The Type 3a event rings in the calamitalean KH0277 (Fig. 7A–D) and the pycnoxylic gymnosperm K1777 (Fig. 7E) differ significantly from other Type 3 rings, because they are associated with a major injury zone. Similar scars have been documented resulting from various causes, such as wildfire, lightning strike, frost event, arthropod frass or different causes of mechanical damage (e.g. Creber and Chaloner, 1984; Schweingruber, 1996; Falcon-Lang et al., 2015). More detailed studies will follow to shed light on the cause of these event zones.

5.4. Plant ecological adaptations

The different plant groups in the Chemnitz Fossil Forest revealed varying plant ecological strategies to droughts, expressed by the various morphological types of tree rings. Pycnoxylic gymnosperms, such as cordaitaleans and conifers show predominantly Type 1 rings, which indicate growth interruptions during dry seasons by their sharp latewood-earlywood boundaries (Figs. 4,5), and thus represent tree rings in the narrow sense (Schweingruber, 1996). In contrast, indistinct but regular Type 2 rings of medullosans and calamitaleans are similar to false rings in the pycnoxylic gymnosperms from Chemnitz as well as in modern trees, where they develop during intra-seasonal droughts (Creber and Chaloner, 1984). As shown by Luthardt and Rößler (2017), correlation of Type 2 ring sequences to Type 1 ring sequences shows a good congruence, demonstrating that Type 2 rings are truly seasonally induced. Thus, it is assumed that growth activity in calamitaleans and medullosans decreased during drier seasons, but did not produce any clear interruption. A major cause of varying tree-ring markedness among different taxa could be leaf longevity, whereas deciduous trees produce sharp rings similar to Type 1 and evergreen trees produce indistinct rings similar to Type 2 (Falcon-Lang, 2000; Falcon-Lang et al., 2014). In modern tropical trees, different tree-ring morphologies show

no relation to leaf fall behaviour or other physiological factors (Coster, 1927, 1928; Worbes et al., 2013). For calamitaleans in the present study, it was demonstrated that they abscised their leafy shoots during droughts (Rößler and Noll, 2006; Rößler and Noll, 2010), whereas medullosans are generally thought to be evergreen (Pfefferkorn et al., 1984). However, both plant groups show indistinct Type 2 rings. Consequently, tree-ring morphology may be no reliable indicator of leaf fall behaviour for the here investigated plant groups.

In basal stem ring sequences from the Chemnitz-Hilbersdorf excavation, growth rates in juvenile stages are as high as in adult stages (Fig. 9). This contrasts to trees in modern forests with closed canopy, which show narrow rings in the juvenile stage due to light deficiency and enhanced competition pressure (Schweingruber, 1996). The canopy at the Chemnitz-Hilbersdorf site was probably not closed, allowing a sufficient portion of sunlight to reach the forest floor and resulting in uninhibited growth of smaller juvenile plants.

Dendroecological evaluation of ring sequences reveals further differences in plant group's physiological behaviour, as well as in their growth rates and thus annual wood production (Fig. 9). Growth rates in trees can vary from trunk to branch to twig, as it was demonstrated by Falcon-Lang (2005b). Nevertheless, annual growth of stem radii exhibits a good correlation to tree radius ($R^2 = 0.77$), as shown in Fig. 9D. The slope of regression curve of 2.86 determines the overall growth rate of the investigated plants and is in good accordance to the total mean ring width of $MW_T = 2.81$ mm. Thus, annual wood production based on radial increments was ca. 2.8 to 2.9 mm/yr. Annual growth rates in modern tropical forests are highly variable in between functional groups of trees as pioneers, light-demanders or shade-bearers, but also due to limiting factors as water, irradiance, nutrients and competition (Baker et al., 2003). In comparison to trees of modern tropical forests (Lieberman et al., 1985; Worbes et al., 2003; Mbow et al., 2013; Groenendijk et al., 2014), plants from the Chemnitz Fossil Forest generally show a rather low total growth rate and smaller growth rate variations among the different species.

5.4.1. Pycnoxylic gymnosperms

Permian conifers and cordaitaleans are usually known as tall trees tolerating sub-humid to semi-arid conditions and thus colonising the upland habitats (e.g. Falcon-Lang and Bashforth, 2004, 2005; Falcon-Lang et al., 2016). In transverse sections from basal stems (e.g. HOG-01, K6044), trends of narrower tree rings from the inner to the outer part of the sections indicate slight growth reduction in diameter with ageing (see Supplement 4). At the same time, trees became more robust against environmental stress as expressed by a slight decrease of annual sensitivity. In comparison to calamitaleans and medullosans, pycnoxylic gymnosperms seemed to be the most drought-tolerant plant group in the ecosystem by exhibiting comparatively low average mean sensitivity (MS = 0.35) and basically showing no Type 3 event rings. However, they were still sensitive and thus an indicator of a stressed environment. Annual wood production rate is constantly high during the whole lifetime of the plants, but differs among specimens (Fig. 9A).

5.4.2. Medullosan seed ferns

Medullosans constitute a major part among tropical hygrophilous plant communities of the late Paleozoic. Hence, there exist a number of medullosan studies, although exclusively from Pennsylvanian wetland environments (e.g. Pfefferkorn et al., 1984; Zodrow, 2002; Wilson et al., 2008; Falcon-Lang, 2009). In contrast, Permian species remain poorly investigated, although they seem to represent an anatomically and ecologically quite diverse group (Weber and Sterzel, 1896; Barthel, 2016). Medullosans usually occupied wetland to seasonally dryland habitats and exhibit a wide range of ecological and ecomorphological attributes in adaptation to their ecological niches (DiMichele et al., 2006). In the Chemnitz Fossil Forest they represent a prominent and morphologically diverse group, which formed the understorey of the forested landscape. Rare forms hitherto assigned to *Medullosa stellata*

(Cotta 1832) var. *lignosa* Weber and Sterzel, 1896 share compact woody stems of diameters ranging from 50 to 330 mm and a small central pith surrounded by extended wood of up to 150 mm thickness. Whereas the few and tiny vascular bundles in the pith show only reduced secondary growth, the comprehensive periphery of loose parenchyma-rich wood offered the chance to recognise repeated growth interruptions. In situ medullosans at Chemnitz-Hilbersdorf site show shallowly dipping root systems, in some specimens combined with an up to 0.40 m long tap root (Luthardt et al., 2016). They are assumed to be evergreen, but probably discarded whole fronds when they were dying (Pfefferkorn et al., 1984).

Tree-ring analysis shows that medullosans possess a higher average mean sensitivity (MS = 0.48) compared to gymnosperms (Fig. 8B). Moreover, they frequently have event rings indicating growth stops and tissue damage due to increased environmental stress that may be linked to droughts. Therefore, medullosans can be regarded as sensitive to environmental impact. Their extended fronds generated large leaf surfaces, which may have caused high rates of evaporation and hence a high sensitivity (Schweingruber, 1996; Worbes et al., 2013). This is further supported by generally large tracheids compared to gymnosperms, suggesting high water conductivity potential (Wilson et al., 2008). The combination of wood anatomical and morphological features could explain their high sensitivity and would show that they were not really well-adapted to local environmental conditions of the forest ecosystem. Slightly lower growth rates of medullosans (Fig. 9B) could be either explained by lower light availability in the understorey or as well by their high environmental sensitivity.

5.4.3. *Calamitaleans*

Calamitaleans from the Chemnitz Fossil Forest belong among the largest and most complete ever found, offering high potential to understand their growth and adaptation strategies as well as their role in the plant community. Together with several Permian *Arthropitys* species from low-latitude Southern Hemisphere floral assemblages (Neregato et al., 2015) the Chemnitz specimens share preferred environments, which can be characterised as mineral soils of widely extended alluvial plains sharply contrasting to the mires and clastic shorelines of the Pennsylvanian wetlands (Falcon-Lang, 2015). Particular specimens of the genus *Arthropitys* from the Chemnitz-Hilbersdorf excavation have been investigated in closer detail (Rößler and Noll, 2006, 2010; Rößler et al., 2014). Arborescent sphenopsids were > 15 m tall trees with extended secondary growth and projecting woody branches that formed a three-dimensional crown architecture (Feng et al., 2012; Rößler et al., 2012). Otherwise calamitaleans exhibited highly branched, extended systems of secondary roots, which were developed down to a depth of > 0.40 m (Rößler et al., 2014; Luthardt et al., 2016).

Increased average mean sensitivity (MS = 0.48) and the occurrence of event rings characterise them as sensitive. Probably due to their small leaves and hence reduced assimilation surface, calamitaleans show lower annual wood production, whereas the investigated specimens revealed only minor variation (Fig. 9C). Compared to pycnoxylic gymnosperms, calamitaleans show similar tracheid size, but a higher parenchyma portion of up to ca. 50%. They occupied one of the upper storeys of the stratified canopy and were thus highly exposed to solar radiation and evaporation. However, calamitaleans have proven to possess several effective drought adaptations. Among these, the ability to shed leafy twigs and therefore reduce transpiration. Additionally, high parenchyma portion in the secondary xylem attributes a higher water storing capacity to calamitaleans and hence a considerable resistance to seasonal droughts (e.g. Rößler and Noll, 2006; Rößler et al., 2012; Neregato et al., 2015). On the other hand, the increased amount of water in stems of calamitaleans, but also of medullosans, probably made them more prone to loss of xylem pressure during drought periods, which caused Type 3b/c event rings.

6. Conclusions

1) For the first time comprehensive tree-ring analyses of arborescent plants were successfully applied to a Permian T[0] assemblage. This study assesses the fourth dimension of a three-dimensionally preserved forest ecosystem grown under seasonal climate on an alluvial plain. Results unravel high-resolution palaeo-environmental development for a period of several decades in the scale of years.

2) Investigated woody plants encompassing pycnoxylic gymnosperms, medullosan seed ferns and calamitaleans exhibit seasonally induced tree rings, which were formed during distinct dry periods under a sub-humid local climate. Tree-ring sequences can be correlated among the specimens within the habitat, due to the T[0] preservational situation of this fossil site.

3) Annual character of tree rings was demonstrated by their morphological features and ring widths, providing evidence for one growing season per year, and to estimate plant's ages and annual rates of wood production. Compared to pycnoxylic gymnosperms, medullosans and calamitaleans show low growth rates probably indicating unfavourable growth conditions.

4) By exhibiting different tree-ring types, the plant groups likely show varying adaptations to seasonal droughts according to their sensitivity and protection strategies. Medullosans and calamitaleans possess a high sensitivity and can be used as good indicators for palaeo-environmental changes and events, whereas the less sensitive pycnoxylic gymnosperms have the best tree-ring record offering the highest dendrochronological potential.

5) So called event rings mark distinct environmental impact on the plants, both induced by severe droughts affecting several specimens in the habitat and individual damage of single trees by an accidental event.

6) Tree-ring analysis illustrates that the forest ecosystem seemed to represent an environmentally stressed habitat, controlled by the major limiting factor of water supply.

Appendix A. Supplementary

Supplementary data to this article can be found online at https://doi.org/10.1016/j.palaeo.2017.09.011.

References

Angiolini, L., Jadoul, F., Leng, M.J., Stephenson, M.H., Rushton, J., Chenery, S., Crippa, G., 2009. How cold were the Early Permian glacial tropics? Testing sea-surface temperature using the oxygen isotope composition of rigorously screened brachiopod shells. J. Geol. Soc. Lond. 166, 933–945.

Ash, J., 1983. Growth rings in *Agathis robusta* and *Araucaria cunninghamii* from tropical Australia. Aust. J. Bot. 31 (3), 269–275. http://dx.doi.org/10.1071/BT9830269.

Ash, J., 1985. Growth rings and longevity of *Agathis vitiensis* (Seemann) Benth. & Hook. F. ex Drake in Fiji. Aust. J. Bot. 33 (1), 81–88. http://dx.doi.org/10.1071/BT9850081.

Ash, S.R., Creber, G.T., 1992. Palaeoclimatic interpretation of the wood structures of the trees in the Chinle Formation (Upper Triassic), Petrified Forest National Park, Arizona, USA. Palaeogeogr. Palaeoclimatol. Palaeoecol. 96 (3–4), 299–317. http://dx.doi.org/10.1016/0031-0182(92)90107-G.

Baker, T.R., Swaine, M.D., Burslem, D.F.R.P., 2003. Variation in tropical forest growth rates: combined effects of functional group composition and resource availability. Perspectives in Plant Ecology, Evolution and Systematics 6 (1,2), 21–36.

Barnett, J.R., 1976. Rings of collapsed cells in Pinus radiate stemwood from lysimeter-grown trees subjected to drought. N. Z. J. For. Sci. 6 (2), 461–465.

Barthel, M., 2016. Die Rotliegendflora der Döhlen-Formation. Geologica Saxonica 61 (2), 105–238 (Senckenberg Naturhistorische Sammlungen, Dresden).

Benício, J., Spiekermann, R., Manfroi, J., Uhl, D., Pires, E.F., Jasper, A., 2015. Palaeoclimatic inferences based on dendrological patterns of permineralized wood from the Permian of the Northern Tocantins Petrified Forest, Parnaíba Basin, Brazil. Palaeobio. Palaeoenv. 96 (2), 255–264. http://dx.doi.org/10.1007/s12549-015-0218-8.

Borchert, R., 1980. Phenology and ecophysiology of tropical trees: *Erythrina Poeppigiana* O. F. Cook. Ecology 61 (5), 1065–1074. http://dx.doi.org/10.2307/1936825.

Bräuning, A., Volland-Voigt, F., Burchardt, I., Ganzhi, O., Nauß, T., Peters, T., 2009. Climatic control of radial growth of *Cedrela montana* in a humid mountain rainforest in southern Ecuador. Erdkunde 63 (4), 337–345. http://dx.doi.org/10.3112/erdkunde.2009.04.04.

Brison, A.-L., Philippe, M., Thevenard, F., 2001. Are Mesozoic wood growth rings climate-induced? Paleobiology 27 (3), 531–538. http://dx.doi.org/10.1666/0094-8373(2001)027<0531:AMWGRC>2.0.CO;2.

Buol, S.W., Hole, F.D., McCracken, R.J., Southard, R.J., 1997. Soil genesis and classification. Iowa State University Press, Ames, IA.

Byers, B.A., Ash, S.R., Chaney, D., DeSoto, L., 2014. First known fire scar on a fossil tree trunk provides evidence of Late Triassic wildfire. Palaeogeogr. Palaeoclimatol. Palaeoecol. 411, 180–187. http://dx.doi.org/10.1016/j.palaeo.2014.06.009.

Césari, S.N., Busquets, P., Méndez-Bedia, I., Colombo, F., Limarino, C.O., Cardó, R., Gallastegui, G., 2012. A late Paleozoic fossil forest from the southern Andes, Argentina. Palaeogeogr. Palaeoclimatol. Palaeoecol. 333–334, 131–147. http://dx.doi.org/10.1016/j.palaeo.2012.03.015.

Chapman, J.L., 1994. Distinguishing internal developmental characteristics from external palaeoenvironmental effects in fossil wood. Rev. Palaeobot. Palynol. 81 (1), 19–32. http://dx.doi.org/10.1016/0034-6667(94)90124-4.

Cook, E.R., Kairiukstis, L.A., 1990. Methods of Dendrochronology. Springer Netherlands, Dordrecht.

Coster, C., 1927. Zur anatomie und physiologie der zuwachszonen- und jahresringbildung in den tropen. Annales du Jardin Botanique de Buitenzorg 37, 49–161.

Coster, C., 1928. Zur anatomie und physiologie der zuwachszonen- und jahresringbildung in den tropen (Fortsetzung). Annales du Jardin Botanique de Buitenzorg 38, 1–114.

Creber, G.T., 1977. Tree rings: a natural data-storage system. Biol. Rev. 52 (3), 349–381. http://dx.doi.org/10.1111/j.1469-185X.1977.tb00838.x.

Creber, G.T., Chaloner, W.G., 1984. Influence of environmental factors on the wood structure of living and fossil trees. Bot. Rev. 50 (4), 357–448. http://dx.doi.org/10.1007/BF02862630.

Creber, G.T., Chaloner, W.G., 1985. Tree growth in the Mesozoic and Early Tertiary and the reconstruction of palaeoclimates. Palaeogeogr. Palaeoclimatol. Palaeoecol. 52 (1–2), 35–59. http://dx.doi.org/10.1016/0031-0182(85)90030-6.

D'Arrigo, R., Wilson, R., Jacoby, G., 2006. On the long-term context for late twentieth century warming. J. Geophys. Res. 111 (D3). http://dx.doi.org/10.1029/2005JD006352.

Denne, M.P., 1989. Definition of latewood according to Mork (1928). IAWA Bulletin 10, 59–62.

Dias-Brito, D., Rohn, R., Castro, J.C., Dias, R.R., Rössler, R., 2007. Floresta Petrificada do TocantinsSetentrional – O mais exuberante e importante registro florístico tropical-subtropical permiano no Hemisfério Sul. In: Winge, M., Schobbenhaus, C., Berbert-Born, M., Queiroz, E.T., Campos, D.A., Souza, C.R.G., Fernandes, A.C.S. (Eds.), Sítios Geológicos e Paleontológicos do Brasil. DNPM/CPRM-SIGEP, Brasília, pp. 14.

DiMichele, W.A., Falcon-Lang, H.J., 2011. Fossil forests in growth position (T⁰ assemblages): origin, taphonomic biases and palaeoecological significance. J. Geol. Soc. Lond. 168 (2), 585–605. http://dx.doi.org/10.1144/0016-76492010-103.

DiMichele, W.A., Tabor, N.J., Chaney, D.S., Nelson, W.J., 2006. From wetlands to wet spots: environmental tracking and the fate of Carboniferous elements in Early Permian tropical floras. Geol. Soc. Am. Spec. Pap. 399, 223–248. http://dx.doi.org/10.1130/2006.2399(11).

Douglass, A.E., 1928. Climatic cycles and tree-growth. In: A Study of the Annual Rings of Trees in Relation to Climate and Solar Activity, Washington. Vol. 2. pp. 166.

Dunlop, J.A., Legg, D.A., Selden, P.A., Fet, V., Schneider, J.W., Rößler, R., 2016. Permian scorpions from the Petrified Forest of Chemnitz, Germany. BMC Evol. Biol. 16 (1), 72. http://dx.doi.org/10.1186/s12862-016-0634-z.

Dunlop, J.A., Rößler, R., 2013. The youngest trigonotarbid *Permotarbus schuberti* n. gen., n. sp. from the Permian Petrified Forest of Chemnitz in Germany. Fossil Record 16

(2), 229–243. http://dx.doi.org/10.1002/mmng.201300012.

Esper, J., Frank, D.C., Timonen, M., Zorita, E., Wilson, Rob J.S., Luterbacher, J., Holzkämper, S., Fischer, N., Wagner, S., Nievergelt, D., Verstege, A., Büntgen, U., 2012. Orbital forcing of tree-ring data. Nat. Clim. Chang. 2 (12), 862–866. http://dx.doi.org/10.1038/NCLIMATE1589.

Eulenberger, S., Tunger, B., Fischer, F., 1995. Neue erkenntnisse zur geologie des Zeisigwaldes bei Chemnitz. Veröff. Mus. Nat. Chem. 18, 25–34.

Falcon-Lang, H.J., 1999. The Early Carboniferous (Courceyan–Arundian) monsoonal climate of the British Isles: evidence from growth rings in fossil woods. Geol. Mag. 136 (2), 177–187. http://dx.doi.org/10.1017/S0016756899002307.

Falcon-Lang, H.J., 2000. The relationship between leaf longevity and growth ring markedness in modern conifer woods and its implications for palaeoclimatic studies. Palaeogeogr. Palaeoclimatol. Palaeoecol. 160 (3–4), 317–328.

Falcon-Lang, H.J., 2005a. Global climate analysis of growth rings in woods, and its implications for deep-time palaeoclimate studies. Paleobiology 31 (3), 434–444. http://dx.doi.org/10.1666/0094-8373(2005)031[0434:GCAOGR]2.0.CO;2.

Falcon-Lang, H.J., 2005b. Intra-tree variability in wood anatomy, and its implications for fossil wood systematics and palaeoclimatic studies. Palaeontology 48 (1), 171–183. http://dx.doi.org/10.1111/j.1475-4983.2004.00429.x.

Falcon-Lang, H.J., 2009. A *Macroneuropteris scheuchzeri* tree preserved in growth position in the Middle Pennsylvanian Sydney Mines Formation, Nova Scotia, Canada. Atl. Geol. 45, 74–80. http://dx.doi.org/10.4138/atlgeol.2009.004.

Falcon-Lang, H.J., 2015. A calamitalean forest preserved in growth position in the Pennsylvanian coal measures of South Wales: implications for palaeoecology, ontogeny and taphonomy. Rev. Palaeobot. Palynol. 214, 51–67. http://dx.doi.org/10.1016/j.revpalbo.2014.10.001.

Falcon-Lang, H.J., Bashforth, A.R., 2004. Pennsylvanian uplands were forested by giant cordaitalean trees. Geology 32 (5), 417. http://dx.doi.org/10.1130/G20371.1.

Falcon-Lang, H.J., Bashforth, A.R., 2005. Morphology, anatomy, and upland ecology of large cordaitalean trees from the Middle Pennsylvanian of Newfoundland. Rev. Palaeobot. Palynol. 135 (3–4), 223–243. http://dx.doi.org/10.1016/j.revpalbo.2005.04.001.

Falcon-Lang, H.J., Cantrill, D.J., Nichols, G.J., 2001. Biodiversity and terrestrial ecology of a mid-Cretaceous high-latitude floodplain, Alexander Island, Antarctica. J. Geol. Soc. Lond. 158 (4), 709–724. http://dx.doi.org/10.1144/jgs.158.4.709.

Falcon-Lang, H.J., Kurzawe, F., Lucas, S., 2014. Coniferopsid tree-trunks preserved in sabkha facies in the Permian (Sakmarian) community Pit Formation in south-central New Mexico, U.S.A.: systematics and palaeoecology. Rev. Palaeobot. Palynol. 200, 138–166. http://dx.doi.org/10.1016/j.revpalbo.2013.09.004.

Falcon-Lang, H.J., Kurzawe, F., Lucas, S.G., 2016. A Late Pennsylvanian coniferopsid forest in growth position, near Socorro, New Mexico, U.S.A.: tree systematics and palaeoclimatic significance. Rev. Palaeobot. Palynol. 225, 67–83. http://dx.doi.org/10.1016/j.revpalbo.2015.11.008.

Falcon-Lang, H.J., Labandeira, C., Kirk, R., 2015. Herbivorous and detritivorous arthropod trace-fossils associated with sub-humid vegetation in the Middle Pennsylvanian of southern Britain. PALAIOS 30, 192–206. http://dx.doi.org/10.2110/palo.2014.082.

Feng, Z., Rößler, R., Annacker, V., Yang, J.-Y., 2014. Micro-CT investigation of a seed fern (probable medullosan) fertile pinna from the Early Permian Petrified Forest in Chemnitz, Germany. Gondwana Res. 26 (3–4), 1208–1215. http://dx.doi.org/10.1016/j.gr.2013.08.005.

Feng, Z., Zierold, T., Rößler, R., 2012. When horsetails became giants. Chin. Sci. Bull. 57 (18), 2285–2288. http://dx.doi.org/10.1007/s11434-012-5086-2.

Fichtler, E., Clark, D.A., Worbes, M., 2003. Age and long-term growth of trees in an old-growth tropical rain forest, based on analyses of tree rings and ¹⁴C. Biotropica 35 (3), 306–317. http://dx.doi.org/10.1111/j.1744-7429.2003.tb00585.x.

Fletcher, T.L., Moss, P.T., Salisbury, S.W., 2015. Wood growth indices as climate indicators from the Upper Cretaceous (Cenomanian–Turonian) portion of the Winton Formation, Australia. Palaeogeogr. Palaeoclimatol. Palaeoecol. 417, 35–43. http://dx.doi.org/10.1016/j.palaeo.2014.10.012.

Francis, J.E., 1984. The seasonal environment of the Purbeck (Upper Jurrasic) fossil forests. Palaeogeogr. Palaeoclimatol. Palaeoecol. 48 (2–4), 285–307. http://dx.doi.org/10.1016/0031-0182(84)90049-X.

Fritts, H.C., 1971. Dendroclimatology and dendroecology. Quat. Res. 1, 419–449.

Glock, W.S., Aegerter, S.R., 1962. Rainfall and tree growth. In: Kozlowski, T.T. (Ed.), Tree Growth. Ronald Press, New York, pp. 23–55.

Glur, L., Stalder, N.F., Wirth, S.B., Gilli, A., Anselmetti, F.S., 2015. Alpine lacustrine varved record reveals summer temperature as main control of glacier fluctuations over the past 2250 years. The Holocene 25 (2), 280–287. http://dx.doi.org/10.1177/0959683614557572.

Groenendijk, P., Sass-Klaassen, U., Bongers, F., Zuidema, P.A., 2014. Potential of tree-ring analysis in a wet tropical forest: a case study on 22 commercial tree species in Central Africa. For. Ecol. Manag. 323, 65–78. http://dx.doi.org/10.1016/j.foreco.2014.03.037.

Gulbranson, E.L., Ryberg, P.E., Decombeix, A.-L., Taylor, E.L., Taylor, T.N., Isbell, J.L., 2014. Leaf habit of Late Permian Glossopteris trees from high-palaeolatitude forests. J. Geol. Soc. 171 (4), 493–507. http://dx.doi.org/10.1144/jgs2013-127.

Haltia-Hovi, E., Saarinen, T., Kukkonen, M., 2007. A 2000-year record of solar forcing on varved lake sediment in eastern Finland. Quat. Sci. Rev. 26 (5–6), 678–689. http://dx.doi.org/10.1016/j.quascirev.2006.11.005.

Harris, E., 1955. The effect of rainfall on the late wood of Scots pine and other conifers in East Anglia. Forestry 28, 136–140.

Kretzschmar, R., Annacker, V., Eulenberger, S., Tunger, B., Rößler, R., 2008. Erste wissenschaftliche grabung im versteinerten wald von Chemnitz - ein zwischenbericht. Freib. Forschungsh. C 528, 25–55.

Larson, P.R., 1963. The indirect effect of drought on tracheid diameter in red pine. For.

Sci. 9, 52–62.

Legler, B., Schneider, J.W., 2008. Marine ingressions into the Middle/Late Permian saline lake of the Southern Permian Basin (Rotliegend, Northern Germany) possibly linked to sea-level highstands in the Arctic rift system. Palaeogeogr. Palaeoclimatol. Palaeoecol. 267 (1–2), 102–114. http://dx.doi.org/10.1016/j.palaeo.2008.06.009.

Lieberman, D., Lieberman, M., Hartshorn, G., Peralta, R., 1985. Growth rates and age-size relationships of tropical wet forest trees in Costa Rica. J. Trop. Ecol. 1, 97–109.

Lima Filho, F.P., 1999. A Sequência Permo-Pensilvaniana da Bacia do Parnaíba. PhD thesis. Programa de Pós-Graduação emGeologia Sedimentar. Universidade de São Paulo, São Paulo, Brasil, pp. 155.

Luthardt, L., Rößler, R., 2017. Fossil forest reveals sunspot activity in the early Permian. Geology 45 (3), 279–282. http://dx.doi.org/10.1130/G38669.1.

Luthardt, L., Rößler, R., Schneider, J.W., 2016. Palaeoclimatic and site-specific conditions in the early Permian fossil forest of Chemnitz – sedimentological, geochemical and palaeobotanical evidence. Palaeogeogr. Palaeoclimatol. Palaeoecol. 441, 627–652. http://dx.doi.org/10.1016/j.palaeo.2015.10.015.

Mbow, C., Chhin, S., Sambou, B., Skole, D., 2013. Potential of dendrochronology to assess annual rates of biomass productivity in savanna trees of West Africa. Dendrochronologia 31 (1), 41–51. http://dx.doi.org/10.1016/j.dendro.2012.06.001.

Montañez, I.P., McElwain, J.C., Poulsen, C.J., White, J.D., DiMichele, W.A., Wilson, J.P., Griggs, G., Hren, M.T., 2016. Climate, p_{CO_2} and terrestrial carbon cycle linkages during late Paleozoic glacial-interglacial cycles. Nat. Geosci. 9, 824–828. http://dx.doi.org/10.1038/ngeo2822.

Morgenroth, E., 1883. Die fossilen pflanzenreste im diluvium der umgebung von Kamenz in Sachsen. Zeitschrift für Naturwissenschaften 1–50.

Mork, E., 1928. Die qualität des fichtenholzes unter besonderer rücksichtnahme auf schief- und papierholz. Papier 26, 741–747.

Neregato, R., Rößler, R., Ianuzzi, R., Noll, R., Rohn, R., 2017. New petrified calamitaleans from the Permian of the Parnaíba Basin, central-north Brazil, part II, and phytogeographic implications for late Paleozoic floras. Rev. Palaeobot. Palynol. 237, 37–61. http://dx.doi.org/10.1016/j.revpalbo.2016.11.001.

Neregato, R., Rößler, R., Rohn, R., Noll, R., 2015. New petrified calamitaleans from the Permian of the Parnaíba Basin, central-north Brazil. Part I. Rev. Palaeobot. Palynol. 215, 23–45. http://dx.doi.org/10.1016/j.revpalbo.2014.12.006.

Opluštil, S., Pšenička, J., Bek, J., Wang, J., Feng, Z., Libertin, M., Šimůnek, Z., Bureš, J., Drábková, J., 2014. T^0 peat-forming plant assemblage preserved in growth position by volcanic ash-fall: a case study from the Middle Pennsylvanian of the Czech Republic. Bull. Geosci. 89 (4), 773–818. http://dx.doi.org/10.3140/bull.geosci.1499.

Parrish, J.T., Peterson, F., 1988. Wind directions predicted from global circulation models and wind directions determined from eolian sandstones of the western United States - a comparison. Sediment. Geol. 56, 261–282.

Pfefferkorn, H.W., Gillespie, W.H., Resnick, D.A., Scheihing, M.H., 1984. Reconstruction and Architecture of Medullosan Pteridosperms (Pennsylvanian). University of Pennsylvania Scholary Commons, pp. 1–8.

Pires, E.F., Guerra-Sommer, M., 2011. Growth ring analysis of fossil coniferous woods from early Cretaceous of Araripe Basin (Brazil). An. Acad. Bras. Ciênc. 83 (2), 409–423. http://dx.doi.org/10.1590/S0001-37652011005000005.

Roscher, M., Berner, U., Schneider, J.W., 2008. Climate modelling – a tool for the assessment of the palaeo-distribution of source and reservoir rocks. Oil Gas European Magazine 34 (3), 131–137.

Roscher, M., Schneider, J.W., 2006. Permo-Carboniferous climate: early Pennsylvanian to Late Permian climate development of central Europe in a regional and global context. Geol. Soc. Lond., Spec. Publ. 265 (1), 95–136. http://dx.doi.org/10.1144/GSL.SP.2006.265.01.05.

Roscher, M., Stordal, F., Svensen, H., 2011. The effect of global warming and global cooling on the distribution of the latest Permian climate zones. Palaeogeogr. Palaeoclimatol. Palaeoecol. 309 (3–4), 186–200. http://dx.doi.org/10.1016/j.palaeo.2011.05.042.

Rößler, R., 2006. Two remarkable Permian petrified forests: correlation, comparison and significance. Geol. Soc. Lond., Spec. Publ. 265 (1), 39–63. http://dx.doi.org/10.1144/GSL.SP.2006.265.01.03.

Rößler, R., Annacker, V., Kretzschmar, R., Eulenberger, S., Tunger, B., 2008. Auf Schatzsuche in Chemnitz - Wissenschaftliche Grabungen '08. Veröff. Mus. Nat. Chem. 31, 5–44.

Rößler, R., Feng, Z., Noll, R., 2012. The largest calamite and its growth architecture — *Arthropitys bistriata* from the Early Permian Petrified Forest of Chemnitz. Rev. Palaeobot. Palynol. 185, 64–78. http://dx.doi.org/10.1016/j.revpalbo.2012.07.018.

Rößler, R., Kretzschmar, R., Annacker, V., Mehlhorn, S., 2009. Auf schatzsuche in Chemnitz - wissenschaftliche grabungen '09. Veröff. Mus. Nat. Chem. 32, 25–46.

Rößler, R., Kretzschmar, R., Annacker, V., Mehlhorn, S., Merbitz, M., Schneider, J.W., Luthardt, L., 2010. Auf schatzsuche in Chemnitz - wissenschaftliche grabungen '10. Veröff. Mus. Nat. Chem. 33, 27–50.

Rößler, R., Luthardt, L., Schneider, J.W., 2015. Der versteinerte wald Chemnitz – momentaufnahme eines vulkanisch konservierten Ökosystems aus dem Perm. Jber. Mitt. Oberrhein. geol. Ver., N.F. 97, 231–266.

Rößler, R., Merbitz, M., 2009. Fenster in die erdgeschichte – die suche nach kieselhölzern auf dem sonnenberg in Chemnitz. Veröff. Mus. Nat. Chem. 32, 47–54.

Rößler, R., Merbitz, M., Annacker, V., Luthardt, L., Noll, R., Neregato, R., Rohn, R., 2014. The root systems of Permian arborescent sphenopsids: evidence from the Northern and Southern hemispheres. Palaeontographica, Abt. B 290 (4–6), 65–107.

Rößler, R., Noll, R., 2006. Sphenopsids of the Permian (I): The largest known anatomically preserved calamite, an exceptional find from the Petrified Forest of Chemnitz, Germany. Rev. Palaeobot. Palynol. 140 (3–4), 145–162. http://dx.doi.org/10.1016/j.

revpalbo.2006.03.008.

Rößler, R., Noll, R., 2010. Anatomy and branching of *Arthropitys bistriata* (Cotta) Goeppert – new observations from the Permian Petrified Forest of Chemnitz, Germany. Int. J. Coal Geol. 83 (2–3), 103–124. http://dx.doi.org/10.1016/j.coal.2009.07.011.

Rößler, R., Zierold, T., Feng, Z., Kretzschmar, R., Merbitz, M., Annacker, V., Schneider, J.W., 2012. A snapshot of an early Permian ecosystem preserved by explosive volcanism: New results from the Chemnitz Petrified Forest, Germany. PALAIOS 27 (11), 814–834. http://dx.doi.org/10.2110/palo.2011.p11-112r.

Rozendaal, D., Zuidema, P.A., 2011. Dendroecology in the tropics: a review. Trees 25 (1), 3–16. http://dx.doi.org/10.1007/s00468-010-0480-3.

Schneider, J.W., Körner, F., Roscher, M., Kroner, U., 2006. Permian climate development in the northern peri-Tethys area – the Lodève Basin, French Massif Central, compared in a European and global context. Palaeogeogr. Palaeoclimatol. Palaeoecol. 240 (1–2), 161–183. http://dx.doi.org/10.1016/j.palaeo.2006.03.057.

Schneider, J.W., Lucas, S.G., Werneburg, R., Rößler, R., 2010. Euramerican Late Pennsylvanian/Early Permian arthropleurid/tetrapod associations – implications for the habitat and paleobiology of the largest terrestrial arthropod. In: Lucas, S.G., Schneider, J.W., Spielmann, J.A. (Eds.), Carboniferous–Permian Transition in Cañon del Cobre, Northern New Mexico, pp. 49–70.

Schneider, J.W., Rößler, R., Fischer, F., 2012. Rotliegend des Chemnitz-Beckens, in: Deutsche Stratigraphische Kommission (Ed.): stratigraphie von Deutschland X. Rotliegend. Teil I: Innervariscische Becken. Schriftenreihe Dt. Ges. Geowiss. SDGG 61, 319–377.

Schollän, K., Karamperidon, C., Krusic, P., Cook, E., Helle, G., 2015. ENSO flavors in a tree-ring $\delta^{18}O$ record of *Tectona grandis* from Indonesia. Clim. Past 11, 1325–1333. http://dx.doi.org/10.5194/cp-11-1325-2015.

Schulz, M., Schneider, J.W., 2015. Sedimentary Cycles and Biota of the Early Permian Wintersbrunnen Lake Horizon, Thuringian Forest Basin, Germany. 86. Jahrestagung der Paläontologischen Gesellschaft, Schiffweiler-Reden, Germany, September 14–16, 2015, Abstract Volume. pp. 49–50.

Schweingruber, F.H., 1996. Tree Rings and Environment Dendroecology. Paul Haupt, Bern, pp. 609.

Schweingruber, F.H., 2001. Dendroökologische Holzanatomie: Anatomische Grundlagen der Dendrochronologie. Paul Haupt, Bern, pp. 472.

Schweingruber, F.H., Börner, A., Schulze, E.-D., 2006. Atlas of Woody Plant Stems: Evolution, Structure, and Environmental Modifications. Springer, Berlin, pp. 229.

Spindler, F., Werneburg, R., Schneider, J.W., Luthardt, L., Annacker, V., Rößler, R., 2017. First Arboreal 'Pelycosaurs' (*Synapsida*: *Varanopidae*) From the Early Permian Chemnitz Fossil Lagerstätte, SE-Germany, With a Review of Varanopid Phylogeny. (Pal Z XXX, XXX–XXX).

Tabor, N.J., Montañez, I.P., 2004. Morphology and distribution of fossil soils in the Permo-Pennsylvanian Wichita and Bowie Groups, north-central Texas, USA: implications for western equatorial Pangean palaeoclimate during icehouse-greenhouse transition. Sedimentology 51 (4), 851–884. http://dx.doi.org/10.1111/j.1365-3091.2004.00655.x.

Tavares, T.M.V., Rohn, R., Rößler, R., Noll, R., 2014. Petrified Marattiales pinnae from the Lower Permian of North-Western Gondwana (Parnaíba Basin, Brazil). Rev. Palaeobot. Palynol. 201, 12–28. http://dx.doi.org/10.1016/j.revpalbo.2013.09.002.

Taylor, E.L., Ryberg, P.E., 2007. Tree growth at polar latitudes based on fossil tree ring analysis. Palaeogeogr. Palaeoclimatol. Palaeoecol. 255 (3–4), 246–264. http://dx.doi.org/10.1016/j.palaeo.2007.06.013.

Vaganov, E.A., 1990. The tracheidogram method in tree-ring analysis and its application. In: Cook, E.R., Kairiukstis, L.A. (Eds.), Methods of Dendrochronology. Springer Netherlands, Dordrecht, pp. 63–75.

Wang, J., Pfefferkorn, H.W., Zhang, Y., Feng, Z., 2012. Permian vegetational Pompeii from Inner Mongolia and its implications for landscape paleoecology and paleobiogeography of Cathaysia. Proc. Natl. Acad. Sci. U. S. A. 109 (13), 4927–4932. http://dx.doi.org/10.1073/pnas.1115076109.

Weber, O., Sterzel, J.T., 1896. Beiträge Zur Kenntnis der Medulloseae. Dreizehnter Bericht der Naturwissenschaftlichen Gesellschaft zu Chemnitz. pp. 44–143.

Wilson, J.P., Knoll, A.H., Holbrook, N.M., Marshall, C.R., 2008. Modeling fluid flow in Medullosa, an anatomically unusual Carboniferous seed plant. Paleobiology 34 (4), 472–493. http://dx.doi.org/10.1666/07076.1.

Worbes, M., 1985. Structural and other adaptations to long-term flooding by trees in Central Amazonia. Amazoniana 9, 459–484.

Worbes, M., 1995. How to measure growth dynamics in tropical trees: a review. IAWA J. 16 (4), 337–351. http://dx.doi.org/10.1163/22941932-90001424.

Worbes, M., 2002. One hundred years of tree-ring research in the tropics – a brief history and an outlook to future challenges. Dendrochronologia 20 (1–2), 217–231. http://dx.doi.org/10.1078/1125-7865-00018.

Worbes, M., Blanchart, S., Fichtler, E., 2013. Relations between water balance, wood traits and phenological behavior of tree species from a tropical dry forest in Costa Rica – a multifactorial study. Tree Physiol. 33 (5), 527–536. http://dx.doi.org/10.1093/treephys/tpt028.

Worbes, M., Staschel, R., Roloff, A., Junk, W.J., 2003. Tree ring analysis reveals age structure, dynamics and wood production of a natural forest stand in Cameroon. For. Ecol. Manag. 173, 105–123.

Zahner, R., 1963. Internal moisture stress and wood formation in conifers. Forest Prod. 13, 240–247.

Zodrow, E.L., 2002. The "medullsoan forest" at the Lloyd Cove Seam (Pennsylvanian, Sydney Coalfield, Nova Scotia, Canada). Atl. Geol. 38, 177–195.